University of Alberta

Tubulin Structure and Implications For the Self Regulation of Microtubules and Their Interaction With Kinesin

by

©

Ellen Crawford

A thesis submitted to the Faculty of Graduate Studies and Research in partial fulfillment of the requirements for the degree of Master of Science

Department of Physics

Edmonton, Alberta

Fall 2002

University of Alberta

Library Release Form

NAME OF AUTHOR: Ellen Crawford
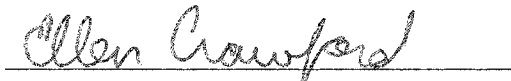
TITLE OF THESIS: Tubulin Structure and Implications For the Self Regulation of Microtubules and Their Interaction With Kinesin

DEGREE: Master of Science

YEAR THIS DEGREE GRANTED: 2002
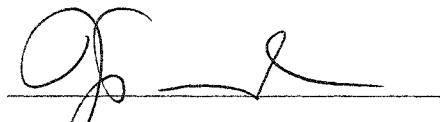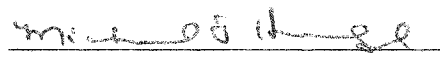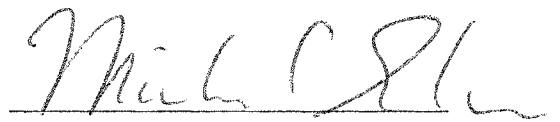
Ellen Crawford
7916 110 Street
Edmonton, Alberta
T6G 1G4

August 8, 2002

University of Alberta

Faculty of Graduate Studies and Research

The undersigned certify that they have read, and recommend to the Faculty of Graduate Studies and Research for acceptance, a thesis entitled **Tubulin Structure and Implications For the Self Regulation of Microtubules and Their Interaction With Kinesin** submitted by **Ellen Crawford** in partial fulfillment of the requirements for the degree of Master of Science.

J.A. Tuszyński (Supervisor)

M.J. Hendzel (External)

M.J. Ellison

R.D. Sydora

DATE:

May 10, 2002

We start off confused and end up confused on a higher level.

Alan Chalmers

Abstract

Tubulin is the main structural protein of the microtubule (MT) cytoskeletal network which forms the mitotic spindle, tracks for intracellular transport, and flagella. Kinesins are motor proteins that use MTs as tracks in these systems.Simulated annealing has been used to predict ATP hydrolysis-induced conformational changes in kinesin's head [44]. I have applied a similar method to tubulin and found that the nucleotide state affected important regions for interdimer contact in the MT lattice.I also placed tubulin in a 2D microtubule lattice and performed simulated annealing on the C-terminii. Both C-terminii resided over β tubulin. The electrostatic potential between a kinesin head and the outer MT surface was then calculated. ADP kinesin was more attracted to tubulin by 2.7 times the ATP hydrolysis energy, in accordance kinesin's MT-binding cycle. The potential minimum was over β tubulin, near the binding site determined by docking calculations [4].

Acknowledgements

Table of Contents

List of Tables

List of Figures

LIST OF FIGURES

LIST OF FIGURES

Chapter 1

Introduction

Biophysics began with scientists who were interested in different types of problems: the biological and the physical. An early example is Helmholtz (1821-1894) who as well as producing the work in electricity and magnetism he is famous for, studied the physiology of vision and hearing. He determined most of the optical parameters for the human eye, still used by optometrists today [17]. In the 1960's the Nobel Prize in Physiology or Medicine went to biophysicists in two subsequent years. In 1962, the prize was awarded for the proposal of the double helix structure for DNA. Two physicists, Crick and Wilkins, teamed up with Watson, a biologist, to solve the problem with x-ray diffraction. The following year, the prize was awarded to Eccles, Hodgkin, Huxley for discovering the ionic mechanisms involved in nerve impulses. The problem was electrical as well as physiological and required knowledge and skill in both fields. Since these pioneering experiments, and others, biology and physics continue to meet in many different ways. Where they were once considered two completely different fields, they have become inseparable in areas such as radiation, spectroscopy (for example NMR), neuroscience, computational biology and more. Cell biophysics is the study of forces acting within and around cells that induce morphogen-

esis, movement or intracellular transport. Molecular biophysics is the study of biomolecules at the atomic level. It involves determining energy of conformations and predicting structures and interactions of biological molecules.

In this project, techniques and ideas from molecular biophysics have been used to learn more about the cell's microtubule network and motor proteins. Microtubules and motor proteins depend on one another to carry out their common functions: cell division, ciliar and flagellar cell movement and intracellular transport. Both the structural components of the cytoskeleton and the capability of movement of the motor proteins are required for all three of these functions. In particular, the atomic structures of tubulin (the constituent protein of microtubules) and the motor protein conventional kinesin are studied. Possible conformational changes and their implications for tubulin self-organization, microtubule stability and tubulin-kinesin interactions are also discussed.

Many models exist for kinesin movement along microtubules. Many of these rely on the interaction between kinesin and the microtubules and the different states of kinesin and sometimes tubulin. With the aid of molecular dynamics software, simulations have been performed on tubulin and kinesin to attempt to find their different conformational states and to study the interaction between the molecules in each state. Different conformations of tubulin have been suggested as a trigger for the dynamic properties of microtubules. As is always the case with molecular systems, they are incredibly complex and many aspects are unknown. There are many different cases to consider and not every situation has been accounted for. One way in which biology and physics seem to clash is the inherent complexity of biological systems and the quest for simplicity and elegance in physics. Physicists studying biology and vice versa are highly motivated to solve the problems at hand, despite the complexity because they recognize the usefulness of physical knowledge in many different fields. As more scientists re-

alize the potential for biophysics, the field of competition grows. However, as physics is applied to more and more biological problems either in the form of experimental or theoretical tools, science and society stand only to gain.

Chapter 2

Cell Biology Background

2.1 Proteins: Molecules for Life

For organisms to stay alive in spite of the laws of thermodynamics, they rely on making energetically unfavourable reactions favourable, at least temporarily. This is achieved primarily by proteins (in particular their subclass of enzymes) and as a result, these molecules are crucial for most biological processes including transport and storage, motion, mechanical support, detecting hormones or harmful molecules, and DNA replication, all of which require an unfavourable reaction to be catalyzed. Proteins are abundant and adopt many different forms even in simple, unicellular organisms. A very simple sketch of an animal cell is shown in Figure 2.1.

2.1.1 Amino Acids are the Building Blocks of Proteins

Amazingly, all proteins on earth are constructed using different numbers and sequences of only 20 amino acids. These small units of protein chains have a central α-carbon atom bound to an amino group, a carboxyl group, a hydrogen atom and a side chain or R-group. At neutral pH, the amino group is basic
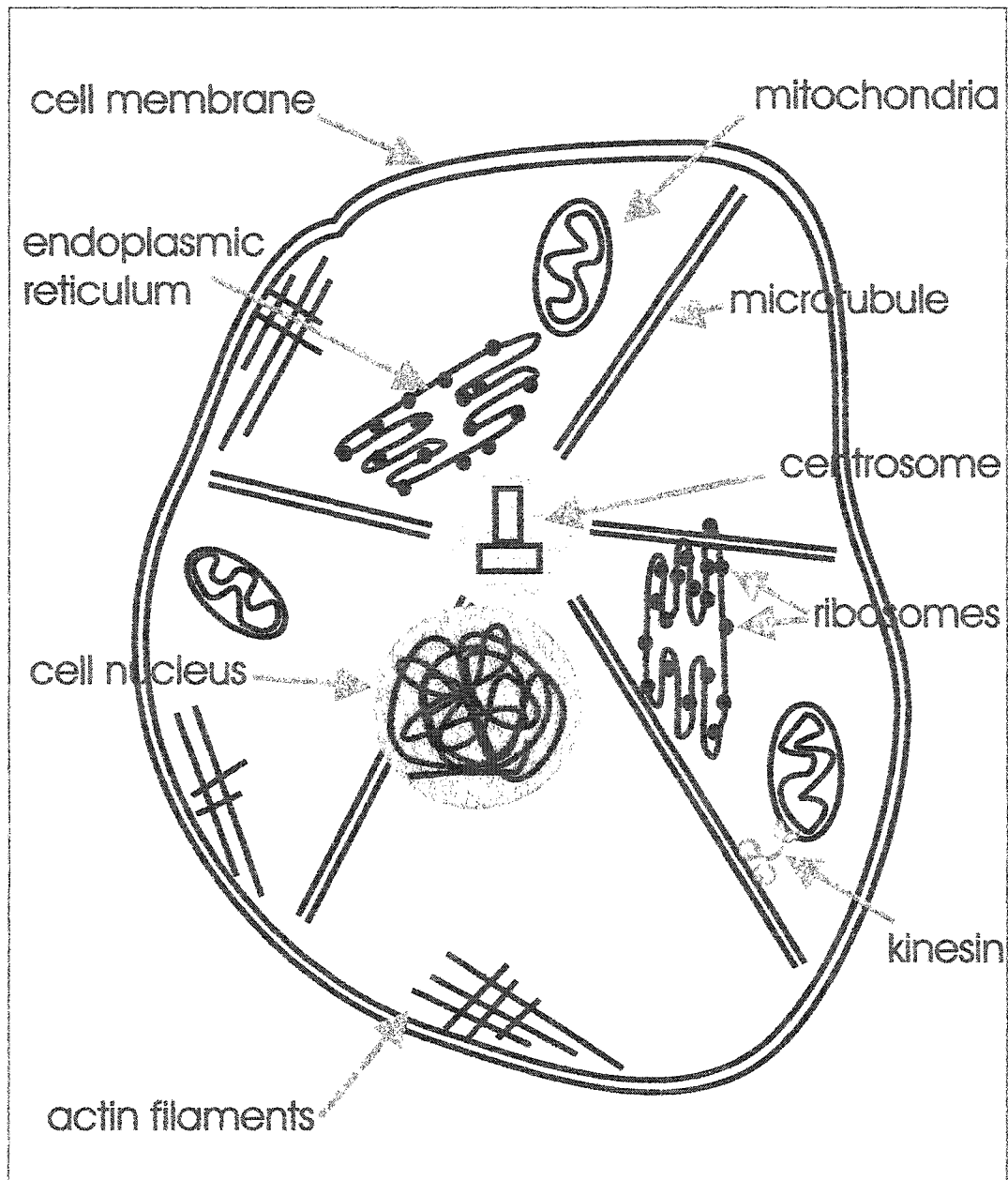
Figure 2.1: Sketch of a generic animal cell
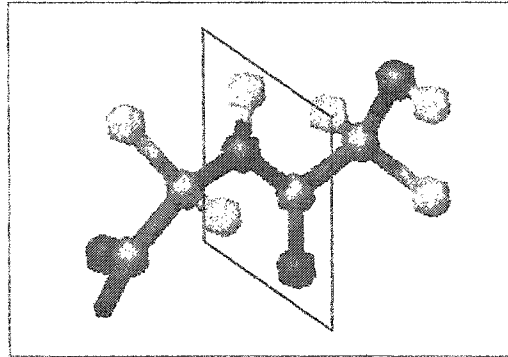
Figure 2.2: In this representation of a peptide bond, the α and central carbon atoms are black, nitrogen atoms are blue, oxygen red, hydrogen white and the first atom of the R-group is green. The planar peptide unit is surrounded by a parallelogram. This figure was created in MOLMOL [25].

and the carboxyl group is acidic, hence the name amino acids. The R-group is distinct for each type of amino acid so they differ in size, shape, charge, hydrogen bonding capability and chemical reactivity. Polarity and charge for each of the 20 amino acids are listed in Table 2.1.

In proteins, amino acids are linked in a chain by peptide bonds between the carboxyl carbon of one and the amino nitrogen of the next so that the resulting polypeptide chain has an N-terminal and a C-terminal end (Figure 2.2). Amino acids in a polypeptide chain are also referred to as residues. The peptide bond is planar and very inflexible. The H on the amino group is always trans, or opposite to, the oxygen on the carboxyl group (with the exception of bonds involving proline) and there is little rotation about the bond because of its partial double bond nature. A large degree of freedom exists about the other two bonds in the chain allowing it to take on a variety of conformations [1, 39].

Table 2.1: The 20 amino acids, their structures, polarity and charges at physiological pH [1].

Name	Symbol	Charge	Polarity
Glycine	Gly or G		Non-Polar R-groups
Alanine	Ala or A		
Valine	Val or V		
Leucine	Leu or L		
Isoleucine	Ile or I		
Proline	Pro or P		
Phenylalanine	Phe or F		
Methionine	Met or M		
Tryptophan	Trp or W		
Cysteine	Cys or C		
Asparagine	Asn or N		Polar R-groups
Glutamine	Gln or Q		
Serine	Ser or S		
Threonine	Thr or T		
Tyrosine	Tyr or Y		
Lysine	Lys or K	+e	
Arginine	Arg or R	+e	
Histidine	His or H	+e	
Aspartic acid	Asp or D	-e	
Glutamic acid	Glu or E	-e	

2.1.2 Protein Structure

The genetic code for a protein determines its amino acid sequence, which is known as its primary structure. Secondary structure of proteins is governed by the particular amino acids in the sequence and tends to be one of three basic motifs. The backbone of the chain (the peptide bonded sequence without the R-groups) can form a spiral cylinder with the R-groups on the outside, known as the α helix (Figure 2.3). Hydrogen bonds between N-H and C-O groups in the backbone fortify this compact structure. In living organisms, the α helix in proteins is always right handed. It is also quite common for two α helices to wind around each other into structure called a coiled coil [1, 39].

The β sheet is another type of secondary structure (shown in Figure 2.4). The constituent β strands are single peptide chains, almost fully extended. They line up beside each other and stabilizing hydrogen bonds between adjacent strands help form a sheet [1, 39].

The most general secondary structure is the random coil where the amino acids are not arranged into any identifiable pattern. Random coil regions form the loops between the helices and sheets in proteins but despite their random nature, can be structurally very important. These flexible regions are often found on the outside of proteins where they are involved in conformational changes and/or substrate binding.

Most proteins are water soluble and their structure tends to be stabilized by having hydrophobic cores. During RNA translation (protein construction) the folding is guided by chaperone proteins but is spontaneous to a large extent. Hydrophobic amino acid side chains are very strongly attracted to each other in the aqueous cytoplasm, thus they tend to amalgamate making possible the existence of large, globular proteins. The internal structure can also be stabilized by sulphur bridges between sulphur-containing residues or hydrogen bonding
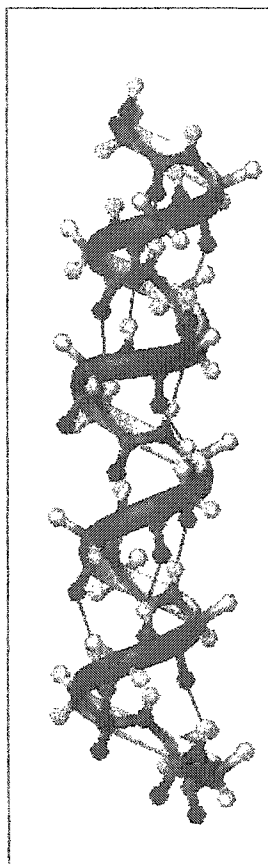
Figure 2.3: α helix: the same colour coding as Figure 2.2 has been used here with a ribbon following the path of the peptide backbone. Hydrogen bonds stabilizing the helix are seen as dotted lines. The green R-groups are on the outside of the helix. The helix used is H10 from α tubulin after it had been subjected to molecular dynamics simulations as described in Chapter 3. This figure was generated with MOLMOL [25].
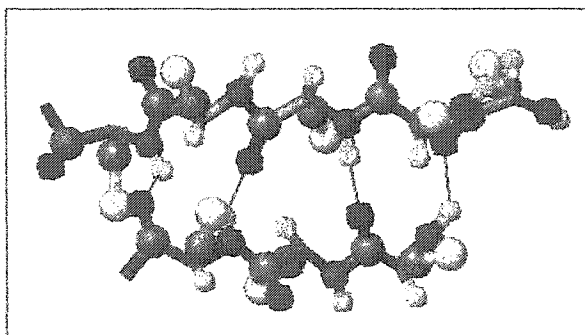
Figure 2.4: This β sheet is also from tubulin (B5 and B6 in β tubulin) and the figure was again generated with MOLMOL [25]. Note that the R-groups in green are perpendicular to the hydrogen bonding (dotted lines) between adjacent β strands in the sheet.

between polar R-groups.

2.1.3 Protein Function

Proteins function by essentially binding a specific molecule (the substrate) which transmits structural changes. There is a wide variety of substrates found in living organisms including oxygen (as in hemoglobin and myoglobin), antigens, DNA, etc. The diversity of structures that can be formed by 20 amino acids allows specialized complimentary clefts or surfaces to be formed for very specific substrate binding. The substrate-protein binding is energetically favourable enough to catalyze an unfavourable reaction which greatly increases the rate at which the reaction occurs.

A common protein substrate is ATP, the cell's easily distributable form of free energy. ATP (adenosine triphosphate) is made with the energy from metabolism and consists of an adenine nucleic base, a ribose and three phosphates. When it is hydrolyzed and loses the third phosphate (creating ADP), 12.5kcal/mol of

energy is released. When compared to other energies at the atomic level, this is quite high. For example, a green photon has an energy of 57kcal/mol, a hydrogen bond is 3 to 7kcal/mol and thermal energy at 310K is 0.6kcal/mol [39]. The high energy nature of the phosphate bond is partly due to the repulsion of the four negative charges in the triphosphate and the lower entropy of a triphosphate relative to a diphosphate and a free inorganic phosphate, P_i. Some enzymes use other nucleotides, GTP, CTP or UTP; that is guanosine, cytosine or uridine triphosphate, respectively. In particular, tubulin uses GTP as its energy source. This allows their action to be regulated separately from ATP binding proteins.

2.2 The Cytoskeleton

Even the cells of seemingly simple organisms are very complex and require many different systems of proteins, sugars, fatty acids and nucleic acids to function and keep the organism alive. One very important system is the cytoskeleton which includes cytoskeletal filaments and motor proteins, among others. The system described here is present in all eukaryotic cells [27]. It is required for cell movement, exo- and endocytosis, cell strength and stability, intracellular transport and cell division. The three types of filaments are actin filaments, intermediate filaments (IFs) and microtubules (MTs). They and their associated motor proteins are described in the sections that follow.

All filaments are made of individual protein monomers which polymerize to form long, strong filaments. They can depolymerize when needed. Motor proteins convert chemical energy into force and motion (for example, for the segregation of chromosomes in mitosis or muscle contraction). They move uni-directionally along cytoskeletal filaments. Individual steps are brought on by conformational changes in the motor domain that are driven by ATP hydrolysis. The motor domains or heads are globular regions connected to an elongated stalk
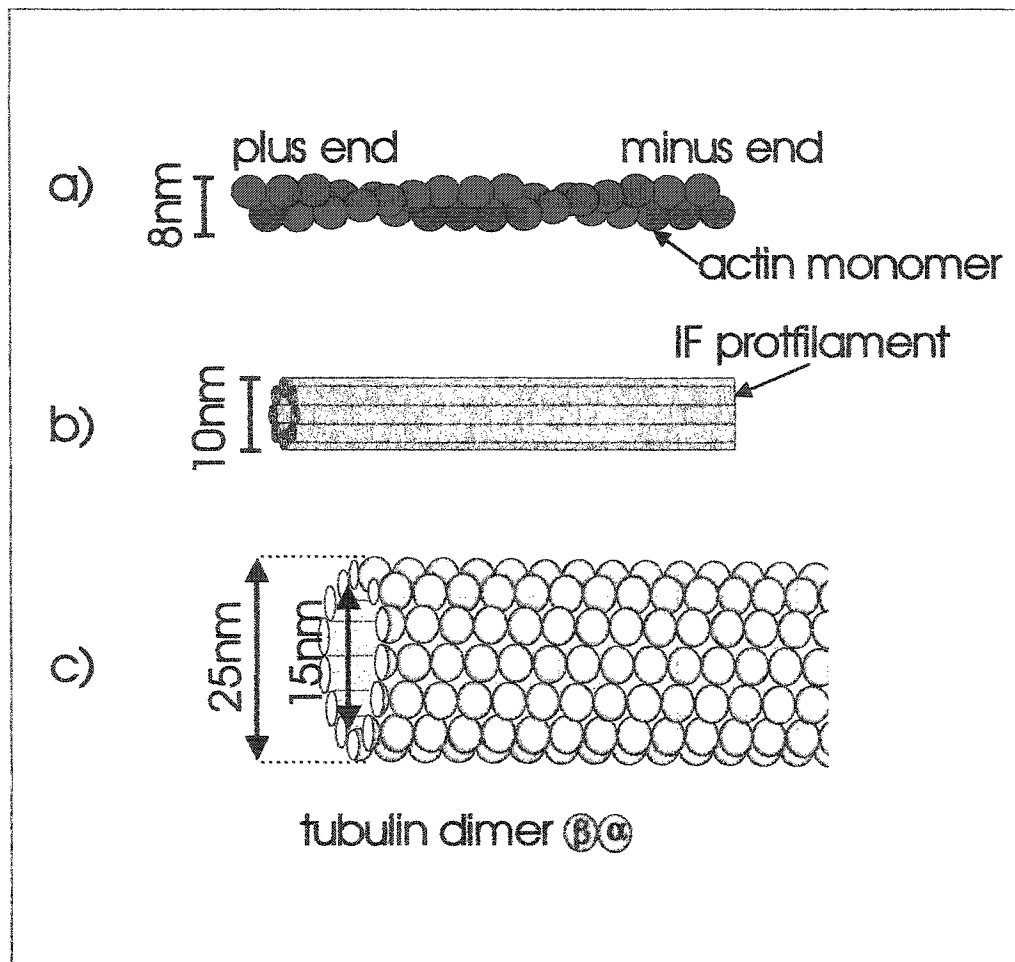
Figure 2.5: Sketches of (a) an actin filament, (b) intermediate filament and (c) a microtubule.

or coiled-coil region which is connected to a tail domain for binding cargo.

Motor proteins are essentially cross-bridges between a filament and a load (which may be another filament). In the case of muscle myosin, the cross-bridges are between thin and thick filaments (formed by the tail domains of the myosins). Dyneins are cross-bridges between MTs in cilia and kinesins bridge adjacent MTs or MTs and organelles/cargo.

2.2.1   Actin Filaments and Myosin

Actin filaments are required to produce forces for many types of cell movement including muscle contraction and relaxation, cytokinesis, and amoeboid motion. These are generally achieved by parallel, antiparallel or crosslinked actin filaments being moved relative to one another by myosins. A network of crosslinked actin filaments also accounts for many viscoelastic properties of the cytoplasm [27].

There are over 60 classes of actin-binding proteins and the number is increasing as more are discovered. They perform functions such as monomer sequestrations, filament severing, capping and crosslinking, motility and interaction with other filaments, MTs, IFs or membrane channels. They regulate the polymerization, depolymerization and higher order assembly of filaments into structures such as lamellopodia.

The globular protein G-actin is the monomeric unit of these filaments. Under physiological conditions, with ATP hydrolysis, it polymerizes into F-actin, the 10nm thick, double helical filamentous form (see Figure 2.5).

Myosin is one type of actin-binding protein and is also a motor protein. Some types of myosin are monomeric and some are dimeric. Sizes of myosins range from 100-310kDa[1]/subunit. Myosins are thought to function by a powerstroke

---

[1]A Dalton (1.0000amu) is a unit of measurement used to describe the mass of proteins.

induced by a conformational change that is part of the ATP hydrolysis, binding and unbinding cycle [22]. Many myosins together are responsible for muscle contraction by sliding actin filaments along each other with an oar-like motion.

2.2.2 Intermediate Filaments

Intermediate filaments are present in the majority of animal cells and can be constructed from 50 different proteins. The building blocks polymerize individually or in groups of two or three to form 10nm-thick filaments [27] as shown in Figure 2.5. The IF network is distributed from the nuclear surface to the plasma membrane and exists on the inside of the nuclear envelope as a karyoskeletal network.

The different types of IF proteins include keratins, neurofilaments, lamins and others. Keratins, which constitute hair and nails in animals are the most abundant structural proteins in epidermal tissues. Neurofilaments are the major determinants of the diameter of axons. Connections between IFs and the membrane, Z discs (in skeletal muscle) and cardiac discs (in cardiac muscle) are very important for maintaining structural integrity during motion. The nuclear lamina seems to be essential for the elongation phase of DNA replication [27].

IFs appear to be responsible for structural integrity of the cell and nucleus during interphase (the part of the cell cycle when the cell is not dividing). They are not as dynamic as actin filaments or, especially, microtubules. The lamins maintain the nuclear shape and architecture but are disassembled and disperse into the cytoplasm as cells enter mitosis. The nuclear lamina is reformed in each of the daughter cells after they have divided. Cytoplasmic IFs tend not to be fully taken apart during mitosis but get segregated into daughter cells by localized phosphorylation and disassembly or localized proteolysis in the growing furrow that cleaves the daughter cells [27].

2.2.3   Microtubules, Dyneins and Kinesins

Unlike the other types of filaments described here, MTs are hollow tubes 25nm in diameter (Figure 2.5). They can grow to be 10 to 100μm in length [14]. They form cilia and flagella in unicellular organisms. MTs are also the structural component of the mitotic spindle. They attach to each chromosome pair, translocate the pairs to the mitotic midplate and during anaphase pull one copy of each pair to the spindle poles. During interphase, when cytoplasmic MTs are not forming the spindle, they extend out from the centrosome towards the extremities of the cell, helping to determine its shape and internal structure, distribute organelles and maintain the intermediate filament array. MTs are also the main structural component of centrioles, the basal body of flagella and the microtubule organizing center (MTOC) for cytoplasmic MTs. The MTOC replicates and becomes the spindle poles for cell division.

Dynein and kinesin are motor proteins specific to MTs. Dyneins attach to the flagellar MTs and drive sliding among them causing a whiplike motion. Mitochondria and vesicles are translocated to the cell periphery and back by kinesins and cytoplasmic dyneins using MTs as tracks.

2.2.4   Tubulin and MT Formation

Microtubules are assembled from heterodimers of α and β tubulin and microtubule associated proteins (or MAPs). Tubulin is a globular protein made up of two subunits of mass 50kDa [39]. The α and β tubulin monomers are very similar in both sequence and 3-dimensional structure (Figure 2.6) and have approximately 450 amino acids each. They both bind GTP but the GTP bound to α tubulin is non-exchangeable (i.e. cannot be hydrolyzed or detached from the tubulin dimer) because it is buried in the interface between the monomers. The GTP on β tubulin is partially exposed at the end of the dimer and is therefore
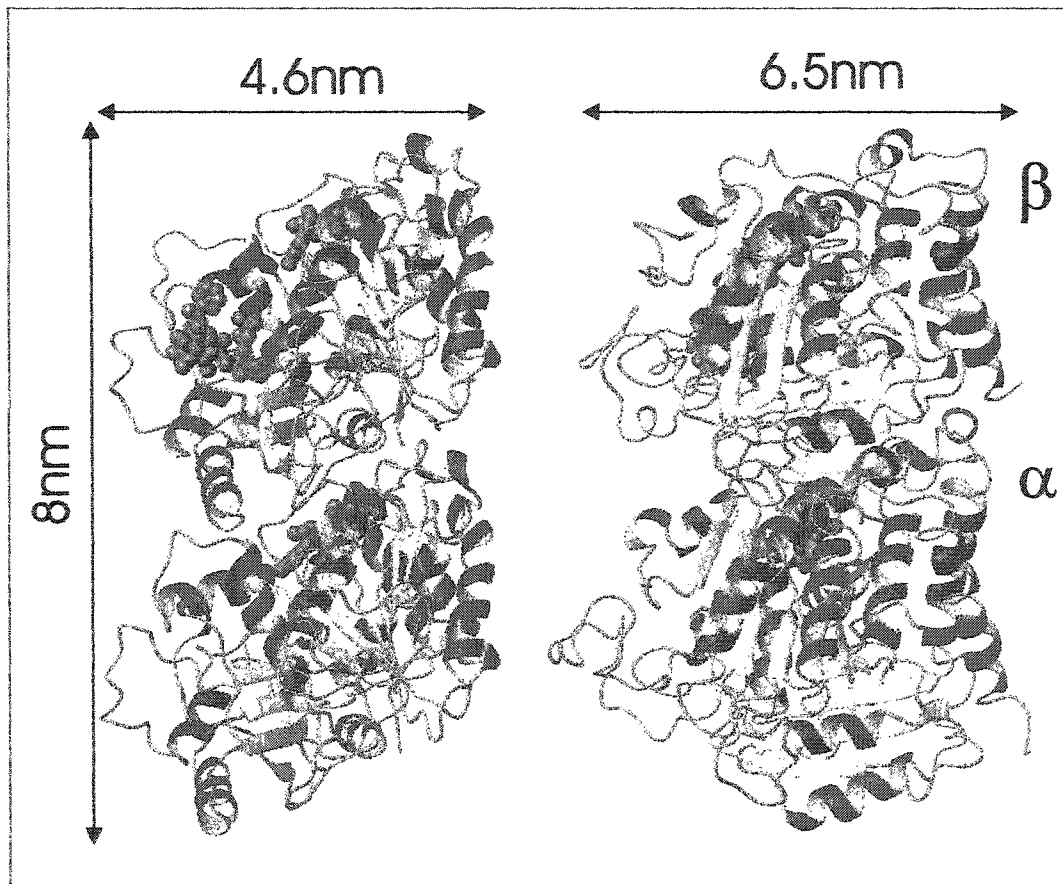
Figure 2.6: A ribbon diagram of the crystal structure of tubulin determined by Nogales *et al.* [35]. The left-hand side is a view of tubulin from the putative inside of the MT, clearly showing the taxotere bound to β-tubulin near the left edge of the molecule. The right-hand side is a side-view of the dimer. The inside of the MT is at the left, and the outside of the MT is at the right where the dimer is very flat. The figure was generated with MOLMOL. [25]

exchangeable [32]. Only tubulin with GTP in the exchangeable site, or E site, can polymerize.

The dimers self assemble end on end to form protofilaments which form cylindrical tubes 25nm in outer diameter (Figure 2.5). MTs usually contain 13 protofilaments joined laterally in a tube. β tubulin is always towards the 'plus end' of the MT, named because it is the growing end. α tubulin is always towards the 'minus end', the end fixed at the centrosome.

The protofilaments are offset from their neighbours by either 0.92nm or 4.92nm so that the array of dimers within the MT is helical. In vivo the more common offset is 0.92nm so that like monomers are attached laterally to each other (Figure 2.5). β-Tu is beside β-Tu and α-Tu is beside α-Tu. In a microtubule with 13 protofilaments, two protofilaments are joined by lateral contacts between unlike monomers (β-α and α-β) in what is known as the seam. MTs like this are said to have tubulin arranged in a B lattice formation. In the less common A lattice, the offset is 4.92nm so lateral connections are between unlike monomers (β-α and α-β) over the entire tube. This lattice pattern does not contain a seam.

An important region of tubulin is the carboxyl terminii of the α and β monomers. These sequences of roughly twelve amino acids rich in negatively charged glutamic acid is on the side of the dimer that makes the outer face of the MT. It is not present in Figures 2.5 or 2.6 because it is very flexible and was not included in the structure by Nogales et al. [35]. It was not resolved because it was too disordered in the tubulin sheets. It is thought to extend out from the surface of the MT and is possibly a very important region because it must interact with anything outside the MT, including motor proteins and microtubule associated proteins or MAPs. It can reach more than 5nm into the cytoplasm [36]. In addition all but one of the many post-translational modifications tubu-

lin undergoes occur at the C-terminus [33]. The results of molecular dynamics simulations on the C-terminus will be described in Chapter 4.

Other types of tubulin do exist, including other isotypes of α and β tubulin and a third type: γ tubulin. γ tubulin is restricted to the MTOCs and is involved in MT nucleation [27].

2.2.5   Microtubule Dynamic Instability

In vitro, MTs have been seen to grow at both ends but growth is three times slower at the minus end than at the plus end [42]. In living cells, the minus ends are fixed at the MTOC so their growth in vivo has not been studied [33]. However in both environments, MT ends seem to be able to switch stochastically between a growth phase and a catastrophic disassembly phase (at rates of around 1.37μm/min and 22.16μm/min respectively [42]) in a process referred to as dynamic instability.

As mentioned earlier, tubulin must have GTP bound to attach to the plus end of a MT. GTP hydrolysis is known to occur at some point after binding but the exact moment at which this occurs is unknown. It is also not known how the energy from hydrolysis is used. The currently favoured model of dynamic instability is the GTP cap model [12, 33]. With GTP bound to β-tubulin, the lateral contacts between β monomers are stronger than with GDP bound. When a tubulin dimer binds to the plus end of a growing MT, the GTP on the second last dimer is hydrolyzed to GDP. Since this dimer is buried in the MT lattice, it does not change conformation even though it is now in an unfavourable conformation for its GDP bound state. Since protofilaments seem to curl and peel apart during catastrophe, it is thought that GDP-Tu has a curved conformation but is kept straight by the lattice [14, 41]. The final layer of dimers has GTP bound to β tubulin with strong lateral contacts between dimers that stabilize

the MT. If it is possible for GTP hydrolysis to be delayed relative to tubulin binding, a multi-layer GTP cap can be formed. But if the reverse occurs or if the GTP cap unbinds from the end of the MT the final layer of dimers will have GDP bound to the β monomer which is incapable of stabilizing a high energy lattice of GDP-tubulin and catastrophic disassembly occurs. Rescues have been observed in which a MT only partially disassembles. These have been explained by the existence of a layer or layers of GTP-tubulin present in the middle of the MT which do not fall apart even when they become exposed, stopping the catastrophe.

The nature and size of the GTP cap is unknown but its existence in at least one layer is well accepted [34]. Dynamic instability depends on the concentrations of GTP and GDP in the cell and probably on the presence of proteins associated with MTs that can induce or suppress stability. The hydrolysis of tubulin regulates the assembly and disassembly of MTs but in the cell there is a host of other proteins associated with tubulin which further regulate the process, from transcription to monomer folding and dimer formation, regulation of α/β tubulin ratios in the cell, post-translational modifications of tubulin, nucleation of MTs, capping and stability that are required for normal function of MTs throughout the cell cycle [33]. The size of the cap depends on whether GTP hydrolysis is required for addition of each new dimer or is simply allowed to occur along with it. This may be influenced by MAPs. It also depends on how stochastic tubulin binding and unbinding can be.

2.2.6 Dyneins

These MT-associated motor proteins are responsible for the beating of cilia and flagella. They also transport cargo along MTs in the minus end direction in axonal transport and mitosis. They can be monomeric, dimeric or trimeric with

subunits of mass 470-530kDa. ATP hydrolysis drives the motion at speeds ranging from $1\text{-}15\mu\text{m/s}$.

2.2.7 Kinesins

Kinesin is another MT-associated motor protein. It is involved in centrosome transport, spindle formation, positioning of chromosomes onto the metaphase plate, transporting organelles and regulating MT dynamics [27]. Conventional kinesin is 360kDa in mass and consists of two heads or motor domains which bind to the outside of the MT, a neck or coiled coil region, connecting the two heads, and a tail which binds whatever load the kinesin is carrying. Kinesin motion is coupled to ATP hydrolysis. ATP-kinesin preferentially binds to the MT and ADP-kinesin binds weakly. Somehow, the heads bind ATP, hydrolyze ATP and release ADP in opposing cycles so that walking is achieved. They move at velocities of a few $\mu\text{m/s}$ and can travel for hundreds of steps without falling off the MT, a characteristic called processivity. The motion is unidirectional always toward the minus end of the MT for conventional kinesin but certain types have plus end-directed motion, for example ncd.

Recent models of kinesin motion depict a hand-over-hand movement along the MT in steps of 8nm, the length of a tubulin dimer [8, 18, 24, 31]. The structural basis of force generation is unknown but probably comes from the necklinker region which attaches the motor domain to the stalk [10, 19]. It is capable of exerting forces up to 5pN [40] and traveling at $2.5\mu\text{/s}$.

None of the cytoskeletal systems described above can function without many chaperone proteins regulating virtually every aspect of their function. Considering the number of systems involved in keeping an entire organism alive, it is not surprising that the number of known proteins in living cells is vast and nowhere near complete. In this thesis a tiny piece of the puzzle is examined in the hopes

of learning more about life as a whole. The approach used involves rigorous computational methods at an atomic level of structural resolution. These methods are used more frequently as an aid to cell biology research and will revolutionize the field in the years to come.

The three-dimensional structure of tubulin determined by Nogales *et al.* [35] in 1998 was at a resolution of 3.7Å. The structure was obtained by electron crystallography of zinc-induced tubulin sheets, formed by the anti-parallel association of protofilaments. This type of sheet therefore has no polarity and can grow in two dimensions, essentially forming a 2D crystal [33]. Taxol stabilizes the sheets against cold and aging. All but the last 10 residues of α tubulin and the last 18 of β tubulin (the so-called C-termini) were included in the structure. Having this structure enables simulations and calculations to be done with tubulin to begin to answer some questions about tubulin itself and its behaviour within microtubules.

Chapter 3

Methods

3.1 Molecular Dynamics Simulations

Molecular dynamics or MD simulations compute the motion of molecules using a set of initial conditions and classical mechanics forces of interaction for the system. These forces include bond length changes, bond angle bending, dihedral angle rotations and nonbonded interactions such as electrostatic or van der Waals forces. Learning more about how a molecule behaves at the atomic level, even if it is by means of a simulation, can give more insight into one of the biggest questions in biochemistry: understanding the relationship between structure and function of proteins. MD can be used as a tool to investigate the structure of molecules, just as experimental techniques such as NMR spectroscopy, X-ray and electron crystallography and photoexcitation measurements etc. are used.

Advantages of using MD include being able to examine flexible parts of molecules for which crystallographic techniques, which rely on a repeating crystal structure, are inappropriate. The main disadvantage of these theoretical techniques is that they are based on classical Newtonian mechanics equations and are thus rather crude approximations of molecules. Also, given current compu-

tational resources, it is often impractical to attempt to mimic living systems or real solutions, especially when studying large proteins like tubulin.

This chapter describes different methods for moving on the potential energy surface of the model. Theoretical results are often a very good accompaniment to experiments either as a means of understanding empirical results or predicting the behaviour of systems.

3.1.1   Energy Minimization

In an energy minimization program, one searches for the minimum energy configuration of a molecule by moving down a gradient through configuration space [43]. This will quickly reach a local minimum because the calculation only goes downhill. It is a useful procedure for relaxing any stretched or high energy conformations in the crystal structure of a protein, for example. This reduces the chance of another simulation moving into an undesired high energy state.

3.1.2   Molecular Dynamics

In molecular dynamics, the kinetic energy of the atoms makes it possible to jump energy barriers on the order of kT and find lower energy regions. A simulation usually consists of integrating Newton's equations of motion to obtain a trajectory, the configuration of the atoms as a function of time [43]. For the ith atom whose Cartesian coordinates are denoted by $\mathbf{r}_i$,

$$\frac{d^2 \mathbf{r}_i}{dt^2} = \frac{\mathbf{F}_i}{m_i} \tag{3.1}$$

where F is the force on atom i. F is determined by the potential, V, which depends on all N atoms in the system,

$$\mathbf{F}_i = -\frac{\partial}{\partial \mathbf{r}_i} V(\mathbf{r}_1, \mathbf{r}_2, .., \mathbf{r}_N). \tag{3.2}$$

The algorithm used to calculate the positions and velocities of the atoms in the system was the Beeman algorithm [5]. Good algorithms for MD combine the need for accuracy of calculations with the limitations in computer time and storage space. The fewer vectors that need to be stored in each cycle of the simulation, the better so multistep methods that use position and velocity values from a previous step or steps to correct predicted values in the current step are preferred [5]. The equations describing the evaluation of position, velocity and acceleration of an atom in the nth time step are

$$
\begin{aligned}
\mathbf{r}_{n+1} &= \mathbf{r}_n + h\mathbf{v}_n + \frac{h^2}{6}(4\mathbf{a}_n - \mathbf{a}_{n-1}) + \frac{h^4}{8}\mathbf{r}_n^{(4)} \tag{3.3}\\
\mathbf{a}_{n+1} &= \frac{-\Delta V(\mathbf{r}_n)}{m}\\
h\mathbf{v}_{n+1} &= \mathbf{r}_{n+1} - \mathbf{r}_n\frac{h^2}{6}(2\mathbf{a}_{n+1} + \mathbf{a}_n) - \frac{h^4}{24}\mathbf{r}_n^{(4)}.
\end{aligned}
$$

These are performed in succession, predicting the position of each atom, evaluating the acceleration and correcting the velocity. In equations (3.3), $\mathbf{r}$, $\mathbf{v}$ and $\mathbf{a}$ are 3D vectors for position, velocity and acceleration, respectively. m represents the molecular mass, and h is the size of the time step. The length of the time step used for calculations is limited by the highest frequency, ν_{max} in the system so that $\Delta t << \frac{1}{\nu_{max}}$. 1fs will be used in the simulations here because the time scale for oscillations of hydrogen atoms in the model system is on the order of 10^{-14}s.

3.1.3 Simulated Annealing

A system as large as tubulin may have many local energy minima so an energy minimization program may not be sufficient to find the lowest global minimum.

To seek the difference in conformation between GTP tubulin and GDP tubulin, a procedure known as annealing was used. The molecule was heated up well beyond physiological temperatures to induce a difference in conformation and was then slowly cooled down below physiological temperatures. If the cooling process is slow enough, the molecule can conceivably move between minima and find a low energy final conformation. This method was applied to kinesin by Wriggers and Schulten [44] and is applied here to tubulin.

3.1.4 Molecular Simulation Software

When modeling molecules, there is a wide range of software packages to choose from. For the work in this thesis, TINKER was used [13]. The advantages of using TINKER include the fact that the source code is easily accessible so that the user can see the algorithms used for calculations and modify them to suit a particular purpose. In addition, the output is not pictorial, it is in terms of numbers whose units are clearly stated so that the output itself can be analyzed easily by the user. In programs with an elaborate graphical interface, the output is often only to the display and the user has little or no control over the calculations. Disadvantages with TINKER are the same as for all molecular modeling software: the accuracy is limited because a model is never an exact representation of a real system. If it were, experimentation would be unnecessary.

3.2 Force Field Parameters

The set of parameters used in the application of potential energy functions is known as the force field. Of the many molecular force fields available, the AMBER force field [9] is used here. The potential function used by the AMBER force field is

$$E_{total} = \sum_{bonds} K_r(r - r_{eq})^2 + \sum_{angles} K_\theta(\theta - \theta_{eq})^2$$
$$+ \sum_{dihedrals} \frac{V_n}{2}[1 + \cos(n\phi - \gamma)]$$
$$+ \sum_{i<j} \left(\frac{A_{ij}}{R_{ij}^{12}} - \frac{B_{ij}}{R_{ij}^6} + \frac{q_i q_j}{\epsilon R_{ij}} \right) \tag{3.4}$$

where K_r, r and r_{eq} are bond force parameter, bond length and equilibrium bond length respectively; K_θ, θ and θ_{eq} are angle force parameter, angle and equilibrium angle respectively; and V_n, n, ϕ and γ are the barrier height, periodicity, angle and phase, respectively for the dihedrals. The nonbonded interactions term is calculated over every pair of atoms i and j. A and B are Lennard-Jones parameters, R_{ij} is the interatomic distance, q_i and q_j are electrostatic charges and ϵ is the dielectric constant [11]. The parameters were fit to small molecules with ab initio quantum mechanical calculations and then adjusted when they had been tested on larger molecules.

Each atom is assigned a specific type with its own parameters. There may be several types to describe one element to account for the number and types of different atoms it can bind to as well as the types of bonds it can be involved in (single, double, etc.). Some atom types used by the AMBER force field are shown in Table 3.1 and a complete list is described in Cornell *et al.* [11]. The bond length and angle bending energies are approximated by simple harmonic oscillator potentials. The dihedral term is represented by the first three terms of a Fourier series. In general, only the n=3 term is used but there are some exceptions. The parameters for most torsion angles depend only on the central atoms and compare well with measurements on low-energy conformations of glycyl and alanyl dipeptides. Both of the nonbonded interactions are calculated only on atoms in different molecules or atoms in the same molecule separated by at least

Figure 3.1: Bond stretching, angle bending and torsional rotation forces used to model the behaviour of molecules.
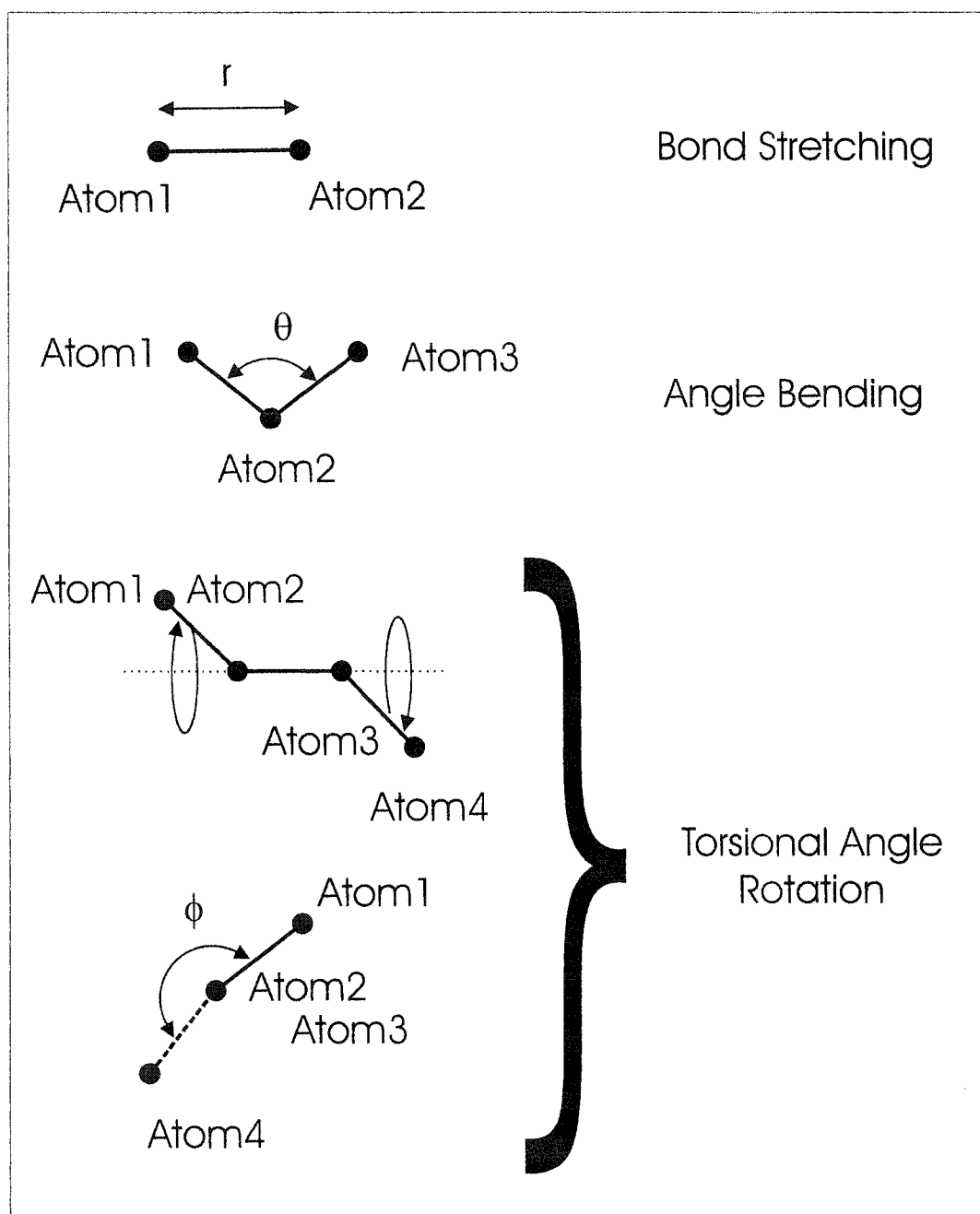
Table 3.1: Some atom types used by the AMBER force field.

atom	type	description
carbon	CT	any sp^3 carbon
	C	any carbonyl sp^2 carbon
	CA	any aromatic sp^2 carbon
nitrogen	N	sp^2 nitrogen in amides
oxygen	OH	sp^3 oxygen in alcohols, tyrosine and protonated carboxylic acids
	OS	sp^3 oxygen in ethers
	O	sp^2 oxygen in amides
	O2	sp^2 oxygen in anionic acids
sulfur	S	sulfur in methionine and cysteine
phosphorus	P	phosphorus in phosphates
hydrogen	H	H attached to N
	HO	H in alcohols and acids
	H1	H attached to aliphatic carbon with one electron-withdrawing substituent

Table 3.2: Lennard-Jones Potential Parameters used in equation (3.5) for selected species [2, 29].

atom	ε(eV)	σ(Å)
Ar	0.0103	3.41
H_2	0.0032	2.93
O_2	0.0102	3.58
C_6H_6	0.0209	8.60

three bonds [9].

The van der Waals interaction in equation (3.4) is represented by the Lennard-Jones potential, depending on the separation of atoms, each atom's van der Waals radius and the well depth for the two atoms involved (see Table 3.2). The typical representation of this potential is

$$V = 4\varepsilon \left[\left(\frac{\sigma}{r} \right)^{12} - \left(\frac{\sigma}{r} \right)^6 \right] \qquad (3.5)$$

where ε is the well depth and σ is the separation between atoms for which $V = 0$. σ is usually roughly the sum of the radii of the two atoms. A and B in equation (3.4) are equal to $4\varepsilon\sigma^{12}$ and $4\varepsilon\sigma^6$ respectively. Thus the attractive term combines dipole-dipole, dipole-induced dipole and induced dipole-induced dipole (or London) forces all of which are proportional to $1/r^6$ [6]. The repulsive term, which is very strong when atoms become too close, was chosen to be proportional to $1/r^{12}$ because it was found empirically to be a reasonable fit to experimental data and it was convenient to use the square of the attractive term in the potential [2, 29]. The AMBER van der Waals parameters for hydrogen atoms take into account the electronegativity of the atom it is bound to, as well as the atoms bound to that atom allowing for a 6-12 potential function to be

Table 3.3: Additional Bond Stretching Parameters for Tubulin

Atom1	Atom2	K_r(kcal/mol/Å^2)	$r_{eq}(\text{Å})$
N	OS	320.0	1.4100
OH	OH	166.0	2.0380

used that closely resembles measured structures and vibrational frequencies.

Electrostatic interactions are represented by the monopole Coulombic term only and each atom type is assigned a partial charge based on this term being the only active one. The partial charges absorb the dipole and other multipole terms in the electrostatic potential. These partial charges were found to reproduce interaction energies, conformational energies and free energies of solvation of simple molecules quite accurately [9].

As with all models, the AMBER force field is an approximation and the aim is to attempt to be as accurate as possible. It is unlikely that biomolecular models will ever completely explain a system, such as a protein, because of their complexity. Even the mathematical complexity of the model system causes difficulties when the number of local energy minima prevents the simulation from properly selecting the global minimum of the system.

3.2.1 Parameters for Nucleotide Binding Proteins

Too many bonds were assigned between tubulin and the nucleotides in the 1TUB.pdb[1] file [7, 35], so the most likely bonds were selected based on the proximity of the atoms in the PDB structure. It was determined that in α-Tu, the

---

[1]The PDB or Protein Data Bank is an online archive for processing and sharing 3D structural data of proteins and other biological macromolecules. As of Nov. 20, 2001 16596 structures of full proteins, partial proteins, DNA, etc. could be found there.

Table 3.4: Additional Angle Bending Parameters for Tubulin

Atom1	Atom2	Atom3	$K_\theta(\text{kcal/mol/rad}^2)$	$\theta_{eq}(\text{deg})$
C	N	OS	50.00	109.50
CT	N	OS	50.00	109.50
C	OH	OH	68.00	103.70
N	CT	OS	50.00	109.50
C	CT	OS	50.00	109.50
N	OS	P	100.00	120.50
OH	CT	OS	45.00	102.60
CT	OH	OH	68.00	103.70

OH of Tyr 224 binds the O2* on the ribose of GTP, both of which are atom type OH. The N of Gly 144 binds one of the oxygens on the γ phosphate of GTP, atom types N and O2 respectively. In β-Tu, CA of Gly 143 binds to an oxygen on the second phosphate of GDP and CB of Ser 178 binds O3* on the ribose of GDP, atom types CT, O2, CT and OS respectively. When GDP was changed to GTP in β-Tu, these bonds were kept the same and the third phosphate was simply added to the molecule. The AMBER parameter set was chosen because it easily accommodates nucleic acids as well as proteins, which is necessary when modeling tubulin and kinesin. However, parameters for bonds between atoms types N and OS and between two atoms of type OH were not included.

Bond stretching, angle bending and torsion parameters were added for the specific bonds between α tubulin and GTP and β tubulin and their attached GDP or GTP that were not available in the AMBER parameter set as it was [9]. The values for these are shown in Tables 3.3, 3.4 and 3.5 . Torsional parameters are often represented only by the two central atoms [11] so for those that were

Table 3.5: Additional Torsional Parameters for Tubulin

Atom				$V_n/2$	γ		$V_n/2$	γ	
1	2	3	4	(kcal/mol)	(deg)	n	(kcal/mol)	(deg)	n
CT	C	N	OS	2.500	180.0	2			
O	C	N	OS	2.500	180.0	2			
C	CT	N	OS	0.000	0.0	2			
H1	CT	N	OS	0.000	0.0	2			
C	N	OS	P	0.380	0.0	3			
CT	N	OS	P	0.380	0.0	3			
CA	C	OH	OH	0.900	180.0	2			
C	OH	OH	CT	3.500	0.0	2	0.600	0.0	3
OS	CT	N	C	0.000	0.0	2			
OS	CT	N	H	0.000	0.0	2			
OS	CT	C	O	0.000	0.0	2			
OS	CT	C	N	0.000	0.0	2			
N	CT	OS	P	0.383	0.0	3			
C	CT	OS	P	0.383	0.0	3			
N	CT	CT	OS	0.156	0.0	3			
OH	CT	OS	CT	0.383	0.0	3			
C	CT	CT	OS	0.156	0.0	3			
OS	CT	OH	HO	0.167	0.0	3			
N	OS	P	OS	0.250	0.0	3	1.200	0.0	2
N	OS	P	O2	0.250	0.0	3			
CT	CT	OH	OH	0.167	0.0	3			
H1	CT	OH	OH	0.167	0.0	3			
CA	C	OH	OH	0.900	180.0	2			

Table 3.6: Cornell and Cannon parameters describing the phosphate dihedrals in GTP and GTP

Param	Atom				$V_n/2$	γ		$V_n/2$	γ	
Set	1	2	3	4	(kcal/mol)	(deg)	n	(kcal/mol)	(deg)	n
Cornell	CT	OS	P	OH	0.250	0.0	3	1.200	0.0	2
	CT	OS	P	OS	0.250	0.0	3	1.200	0.0	2
	P	OS	P	OS	0.250	0.0	3			
	P	OS	P	O2	0.250	0.0	3			
Cannon	CT	OS	P	OH	0.980	0.0	3	1.200	0.0	2
	CT	OS	P	OS	0.980	0.0	3	1.200	0.0	2
	P	OS	P	OS	2.500	0.0	3			
	P	OS	P	O2	2.500	0.0	3			

missing, torsion records that had the correct central atoms were used.

The AMBER parameter set also does not deal with di- or triphosphates so parameters for corresponding angle and torsion parameters were required. The existing angle parameters were found to be appropriate but according to Cannon [9] the torsion parameters present did not accurately describe the GTP molecule according to semiempirical calculations and crystallography. The torsional parameters involving the atoms in question were changed accordingly (Table 3.6).

3.3   Simulated Annealing on Kinesin

TINKER's anneal program was used to heat the proteins up from 1K to 400K for tubulin and from 1K to 500K for kinesin and then cool them very slowly to 200K. Anneal performs molecular dynamics calculations on the molecule while

it is coupled to an external temperature bath.

Figure 3.2: Displacement vs. residue number for ATP·Kin and ADP·Kin after simulated annealing. A mean difference in position of at least 5Å occurs within L5 (residues 94-100), H2 (85-93), H3 (101-116), L9 (187-199), L10 (211,218), L11 (235-251) and L12 (268-277).
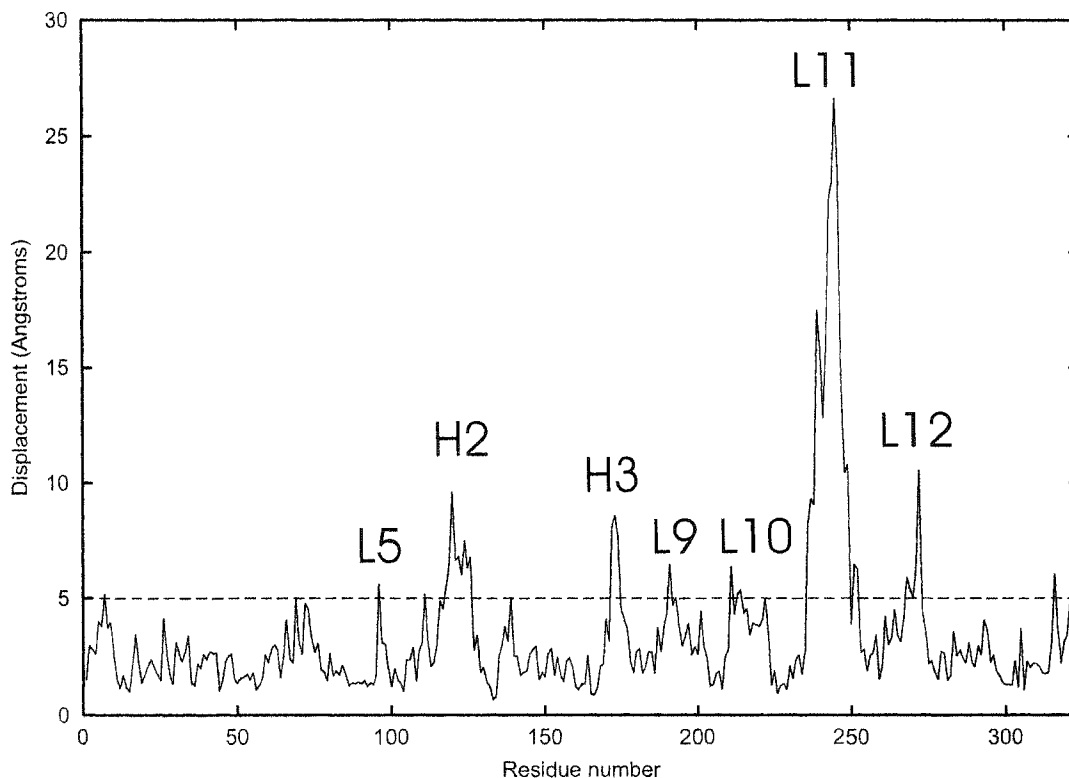
To model the conformational change of a protein requires a great deal of computational time and disk space. But, in the case of kinesin where only the ADP form and not the ATP form of the motor domain has been crystallized, such a computation can be useful. Wriggers and Schulten [44] performed molecular dynamics simulations on the kinesin motor domain or head group while slowly heating the system from zero to 500K and then back down to 200K, in a procedure called simulated annealing. At the higher temperatures, the system can cross potential barriers between minima on the analytical energy surface and cross

Figure 3.3: Changes in the MT binding regions of (a) ADP-Kinesin and (b) ATP-Kinesin brought about by simulated annealing. Atoms in the nucleotides are drawn as spheres and the protein chain is drawn in the ribbon representation. The very flexible L11 along with H4 and L12 are highlighted. This figure was generated with MOLMOL [25]
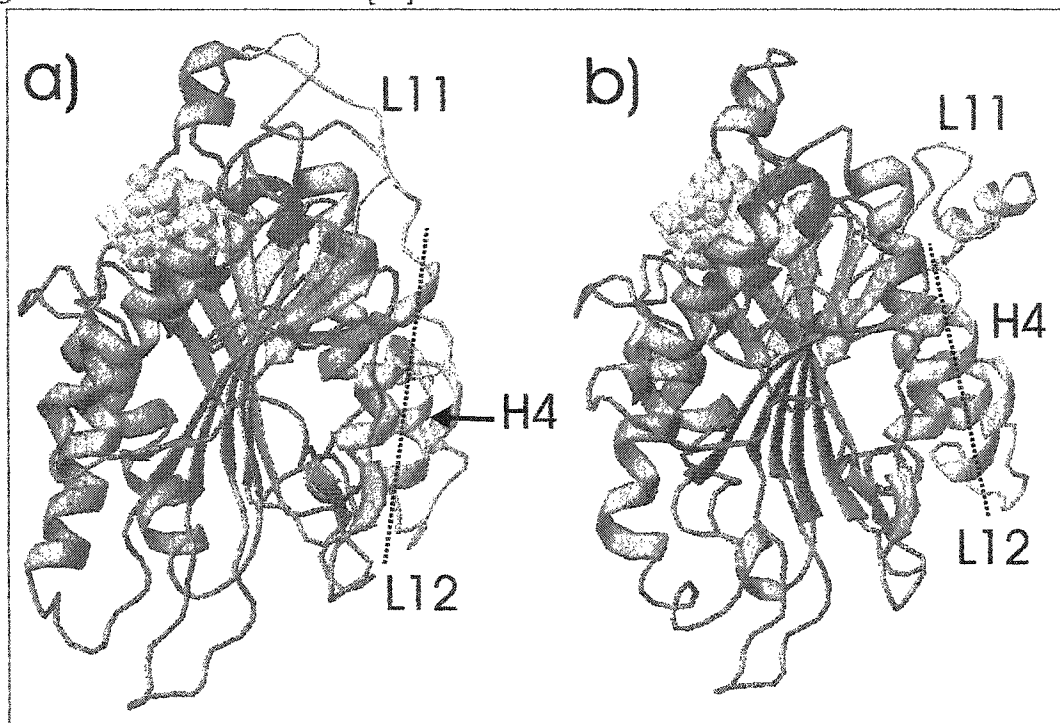
them faster than in a simulation at room or physiological temperatures. The very slow cooling allows the system to stay at the high temperatures for a longer time.

Kinesin was thus used as a test system for TINKER's anneal program. The annealing was repeated but without adding the extra water molecules that Wriggers and Schulten had included [44]. Kinesin's motor domain (structure obtained from Protein Data Bank file 1BG2.pdb [7, 28]) was heated from zero to 500K over 50000ps and then cooled to 200K over 120000ps with time steps of 1fs. The dielectric constant was 1.0 and the cutoff for van der Waals and electrostatic

Figure 3.4: Movement of H3 in kinesin after simulated annealing a)ADP·Kin relative to b)ATP·Kin, figure generated with MOLMOL [25]
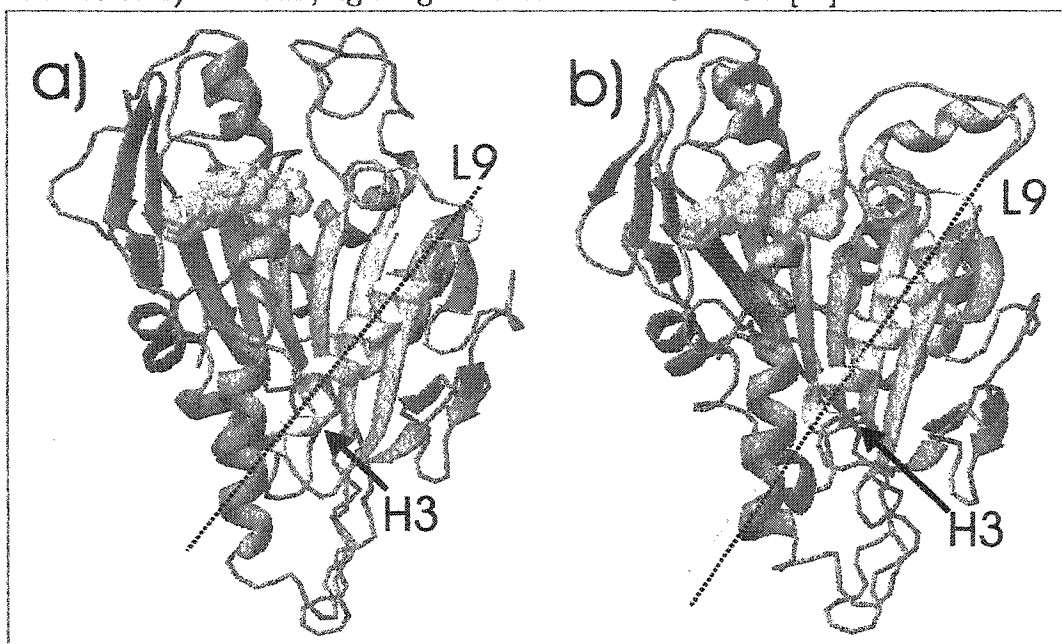
interactions was set to 12.0Å in order to decrease computation time. A distance constraint was used to keep ATP oriented properly by Wriggers and Schulten [44] and is used again here. The γ-phosphorous of ATP and the α-carbon of Gly-234 were constrained within 3.8 and 4.0Å with a force constant of 5.0kcal/Å^2. The difference in position of each atom in the ATP·Kin file relative to the same atom in the ADP·Kin file was then determined and averaged within each amino acid residue to obtain displacement vs. residue data (see Figure 3.2).

Most of the movement occurs in the alpha helices and the loops on the outside of the motor domain, the core of beta sheets is quite stable. Putative MT binding regions are loops L8, L11, L12 and helices H4 and H5. As can be seen by visually examining the molecules some changes that were not apparent in Figure 3.2 are visible. Figure 3.3 shows a bend and a change in angle of helix H4 brought about by the change in L11. The loop L11 is very flexible and thus the extent

of movement seen here should not be taken as a firm conformational change. It is likely that, in vivo, L11 takes on a variety of conformations that depend on kinesin's environment. The subsequent effects on H4 and L12 are more reliable and are similar to what has been seen before [44]. In ATP·Kin in Figure 3.3 (b), L11, H4 and L12 seem to form a more concave MT binding region relative to ADP·Kin in (a) where the shape of the region is more convex. It can be imagined that this is more favourable to MT binding.

Since the results here are similar to those obtained by Wriggers and Schulten [44] simulated annealing was applied to tubulin with and without the C-terminus and on the C-terminus alone.

3.4 Simulated Annealing on Tubulin

Tubulin with its C-terminii will be referred to as tubulin·C and tubulin without the C-terminii will be referred to tubulin when discussing the simulations performed here. tubulin·C was generated by adding the missing residues [35] onto α and β tubulin in MOLMOL [25]. For simulated annealing, the structure files for GDP·Tu·C, GTP·Tu·C, GDP·Tu and GTP·Tu were first minimized in TINKER [13] to a RMS gradient of 0.01. Again the dielectric constant was set to 1.0 and the cutoff for van der Waals and electrostatic interactions was set to 12.0Å. Tubulin became very disordered after 400K so the system was heated from 0K to 400K over 50000ps and cooled to 200K over 120000ps. This way, both the maximum temperature and the change in temperature over time were reduced, preventing denaturation of the protein. The final structures were then minimized again to a RMS gradient of 0.01. In spite of this, GDP·tubulin·C continued to become very disordered near the beginning of the simulated annealing. The atoms HG of β tubulin serine 176 and O3* on the ribose of GDP seemed to be the cause of the problem. After unsuccessfully using minimization or MD

to get the atoms in a lower energy conformation to start the simulated anneal-
ing, they were simply made inactive and simulated annealing was performed on
all atoms of GDP tubulin-C except these two. After the runs were complete,
both molecules were aligned to the axes of the moment of inertia and translated
to the origin to compensate for any rotation or displacement during simulated
annealing.

Chapter 4

Results

One of the many uncertainties surrounding tubulin and MTs is the extent of the structural change in tubulin transmitted from GTP hydrolysis and its effects on MT stability. It has been suggested that the lateral contacts between β tubulin monomers can weaken after the GTP in β tubulin has lost its third, or γ, phosphate [33]. This could explain how a GTP cap might hold the MT together. In this chapter, a solution to this problem is sought using molecular dynamics coupled with a temperature bath on the tubulin dimer to find possible conformational changes resulting from GTP hydrolysis.

Since tubulin's 3D crystal structure of was found with taxol-stabilized sheets [35], the lateral contacts present were not indicative of the situation in a microtubule. When this crystal structure was docked onto a 20Å reconstruction on a MT, information about lateral contacts between dimers was obtained [34]. Nogales et al. found that the lateral contacts between tubulin dimers was dominated by the interaction of residues 279 to 287, the M loop with the H1-B2 loop and helix H3. They proposed that since the loop preceding helix H3 is involved in binding the γ phosphate that in β tubulin·C a conformational change in H3 could be induced by the interaction of this loop with the phosphate. H7 has

also been put forth as a possible transmission agent of energy released during hydrolysis to a conformational change in loop H7-H8, which, in α is involved in longitudinal contacts and in β contact the αGTP [3, 4]. These ideas will be a theme in the discussion that follows.

4.1   Simulations on tubulin·C

When first looking at the displacement vs. residue number graphs in Figure 4.1, the dominant feature in α and β tubulin·C is their C-terminii. In the ribbon diagrams of GTP·Tu·C and GDP·Tu·C in Figures 4.3 and 4.4, the carboxyl terminii have clearly adopted very different positions but this is expected from such a flexible element outside the a protein's globular domain. So, without the C-terminii, the average displacement of the residues of Tu·C is 4.1Å. Residues that had moved less than this average were deemed stable after simulated annealing with either GTP or GDP in the E-site.

The locations and functions of these stable regions are summarized in Table 4.1[1] Regions of a protein might be stable because they are physically confined in space by surrounding residues or are held fixed by electrostatic or van der Waals interactions with neighbouring regions. As a result, they correspond mostly to the core β sheets of the molecule, or to loops or helices that are buried in the middle of the molecule and thus have restricted movement, as in kinesin (Section 3.3). Exceptions to this are highlighted in Table 4.1 and are the sequences that correspond to the middle of H2-B3, the middle of B3-H3, the second half of H3, the first half of H4, the end of H5, the second halves of H8 and H9, the beginning of H11 and the end of H12. Most difficult to explain are the first two loops:

---

[1]For this and all tables in this section, when a structural element in question is on the outside of a tubulin monomer, its position in terms of lateral or longitudinal contacts are from the designations made by Nogales *et al.* in their high resolution model of a microtubule [34].
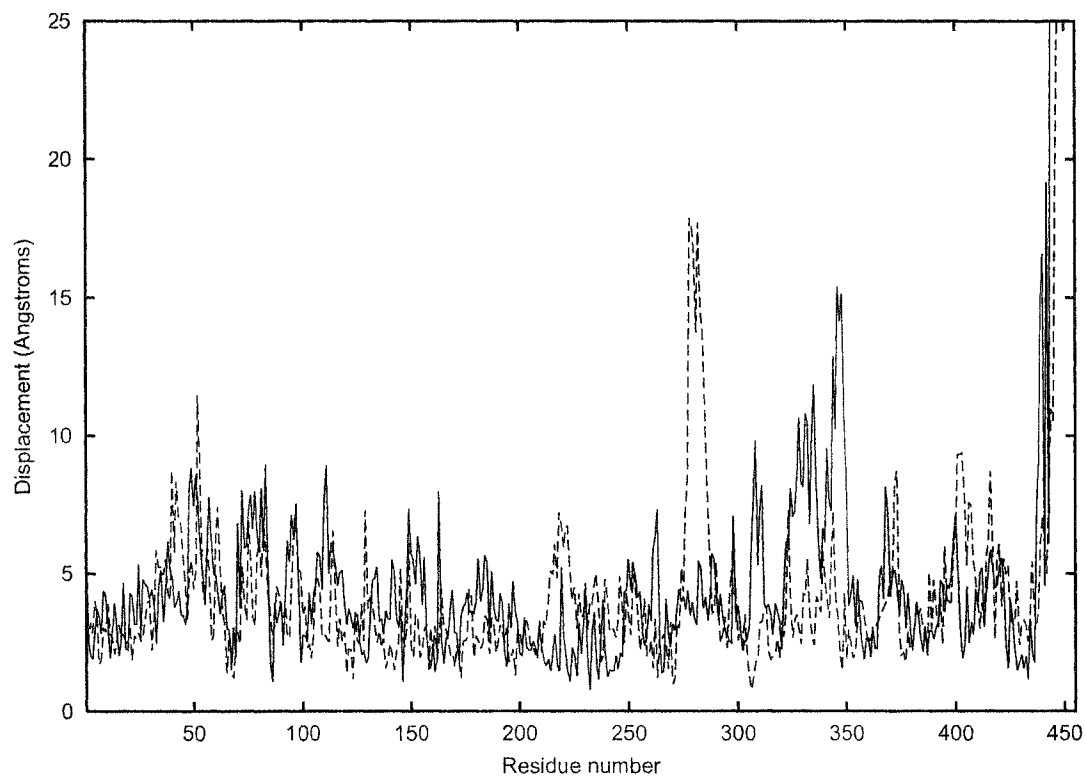
Figure 4.1: Displacement vs. residue number for GTP·Tu·C and GDP·Tu·C after simulated annealing. The solid line represents displacement for α tubulin·C and the dashed line is for β tubulin·C.

Table 4.1: Stable regions in α and β tubulin-C, based on Figure 4.1 Regions in bold font are those that are not buried within the globular domain.

Residues	Structural Element(s)	Location
2-8	B1	β sheet 1
11-17	1st half H1	buried
65-69	B2	β sheet 1
85-87	**middle H2-B3**	**lateral contacts**
100-103	**middle B3-H3**	**side of dimer, long. contacts in β**
119-128	**2nd half H3**	**lateral contacts**
135-140	B4	β sheet1
157-162	**2nd half H4**	**side of dimer**
165-167	B5	β sheet1
170-175	start of B5-H5	buried
192-196	**end of H5**	**side of dimer**
198-213	B6,H6	buried
236-238	2nd half H7	buried
241-245	1st half H7-H8	between β sheets 1 and 2, near B9-B10
256-260	**2nd half H8**	**buried in β, long. contacts in α**
264-272	B7	β sheet 2
293-296	**2nd half H9**	**lateral contacts**
300-305	part of H9-B8	buried
312-320	B8	β sheet 2
356-364	start B9-B10	between β sheets 1 and 2, near H7-H8
379-387	**end B10, start H11**	**outside of MT**
429-434	**end of H12**	**outside of MT**
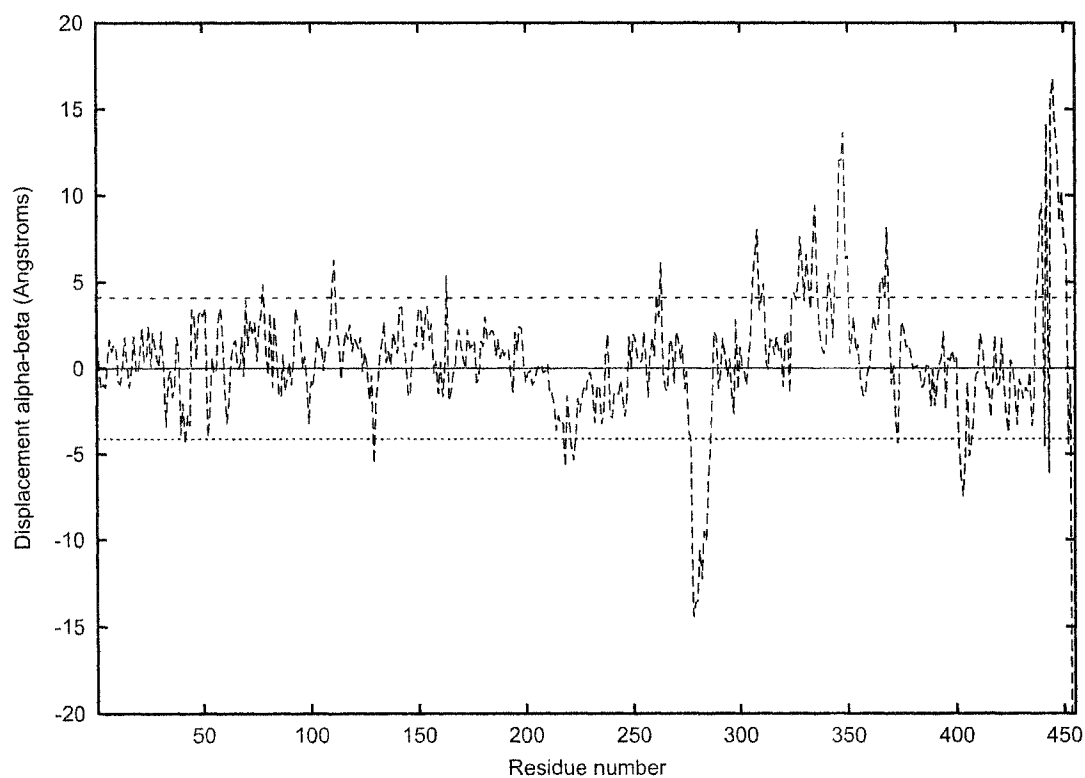
Figure 4.2: β-Tu·C displacement subtracted from α-Tu·C displacement of the data in Figure 4.1 so that negative values represent areas where β-Tu·C has moved more and positive values represent areas where α-Tu·C has moved more.

Table 4.2: Flexible regions in α tubulin·C only, based on peaks that are positive in Figure 4.2.

Residues	Structural Element(s)	Location
75-79	H2	inside of MT
107-113	B3-H3	side of dimer
163	H4-B5	lateral contacts
260-263	H8-B7	side of dimer
305-312	H9-B8	lateral contacts
324-337	H10	lateral contacts/longitudinal contacts
340-351	H10-B9	longitudinal contacts

Table 4.3: Flexible regions in β tubulin·C only, based on peaks that are negative in Figure 4.2.

Residues	Structural Element(s)	Location
40-44	H1-B2	inside of MT
127-131	H3-B4	intradimer contacts
211-229	end H6, H6-H7, start H7	lateral contacts
276-287	B7-H9 or M loop	lateral contacts
372-373	B9-B10	taxotere binding region, inside of MT
401-409	H11-H12	longitudinal contacts

H2-B3 and B3-H3. They are both roughly twelve-residue-long loops outside of the globular domain yet have changed position very little after the simulated annealing. The sequences are both a mixture of charged, polar uncharged and nonpolar residues so the interactions keeping them stable must be very complex as with all interactions in such a large protein. More tests must be done to determine the nature of interactions preventing these areas from being displaced after a temperature increase to 400K. Neither helix H3 nor loop H7-H8, areas that were suggested to be possible locations for conformational change [4, 34] moved significantly after simulated annealing.

Peaks above 4.1Å in Figure 4.1 that are shared by α and β tubulin·C are likely to be due to regions that are quite flexible, like the C-terminus. The only other such regions are between roughly residues 25 and 60 and residues 70 and 85 which includes the H1-B2 loop, H2 and the H2-B3 loop. The loops in this part of the sequence are situated on the inside of the MT and are a flexible region. MT function is uninhibited by amino acid substitutions in this part of the sequence [35]. All four of these regions are coloured red in Figures 4.3 to 4.5.

Peaks that appear in one monomer and not the other might stem from the lack or presence of the γ phosphate in β tubulin·C and reflect hydrolysis-induced conformational changes and can be seen in Figure 4.2. It is also possible that the peaks that are not shared are simply from differences between the monomers but may still provide insight into tubulin·C function. The peaks where the difference in displacement between α and β tubulin·C is greater than the average 4.1Å are summarized in Tables 4.2 and 4.3. The regions in these tables are more often involved in lateral or longitudinal contacts than those in Table 4.1.

The structural elements highlighted in Figures 4.3 to 4.5 are described below. Loop αB3-H3 is on the side of the dimer and is coloured green in Figure 4.4. The end closest to H3 is bent away from the inside of the MT in GTP·Tu·C. Lysine

Figure 4.3: GDP (top) and GTP (bottom) tubulin·C after simulated annealing. The side facing the inside of the MT is at the top. Regions of interest are coloured and labelled. Figure generated with MOLMOL [25].

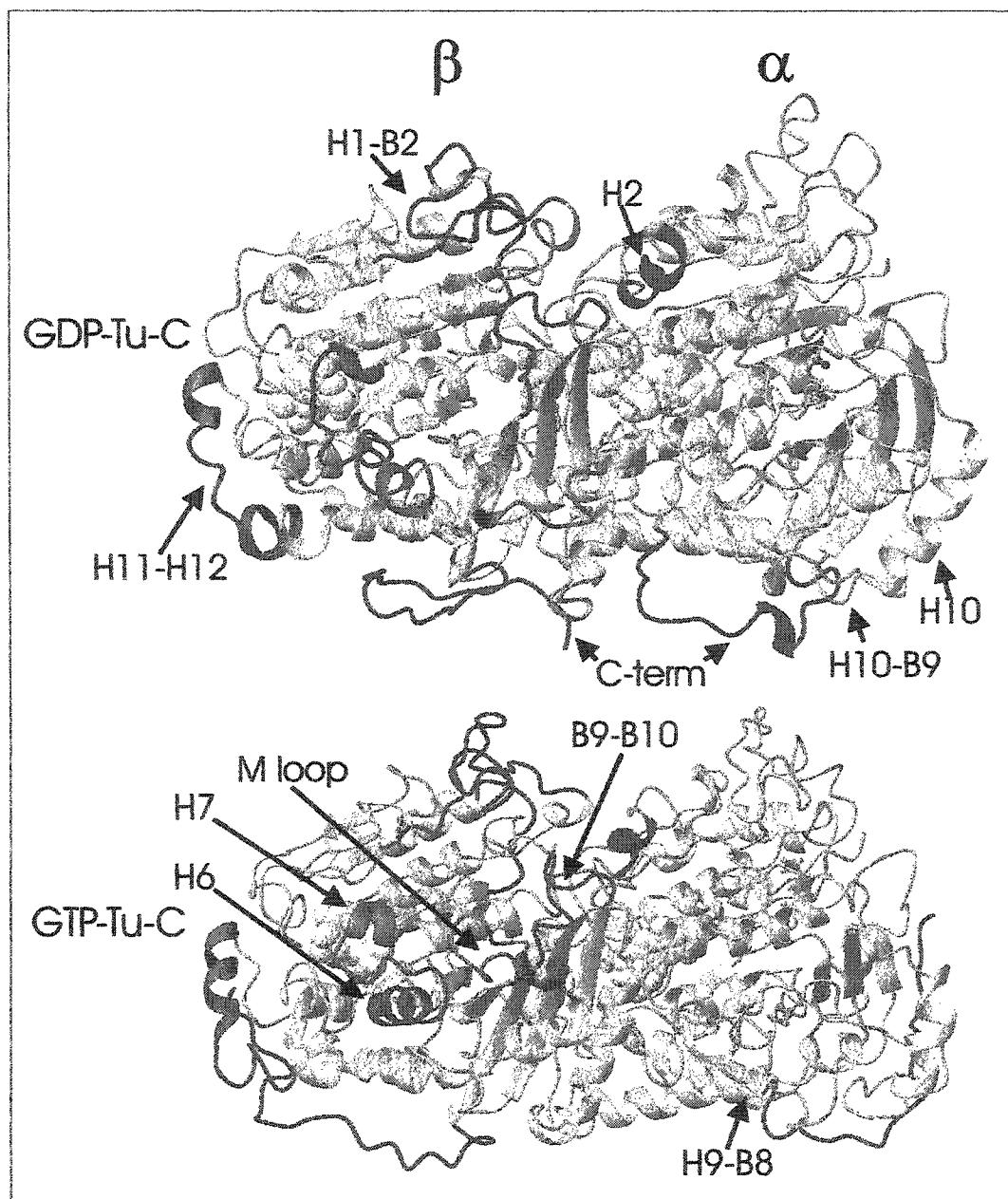Figure 4.4: GDP (top) and GTP (bottom) tubulin·C from the opposite side after simulated annealing. The side facing the microtubule's inside is at the top. Figure created using MOLMOL [25].
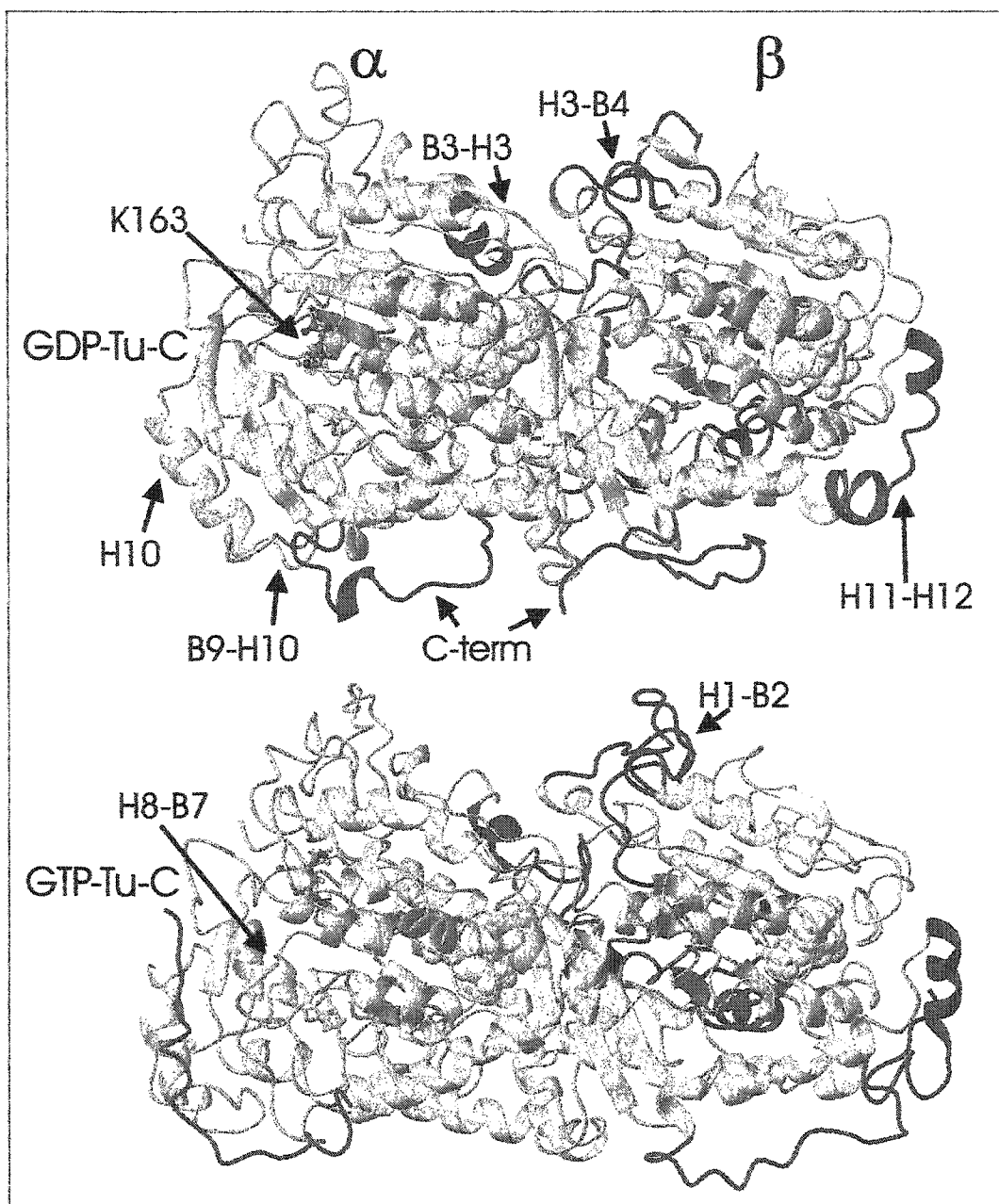
Figure 4.5: GDP (left) and GTP (right) tubulin-C looking at the β end of the molecule. The side facing the inside of the MT is at the top. Colouring is the same as in Figure 4.3 and this figure was again generated using MOLMOL [25].
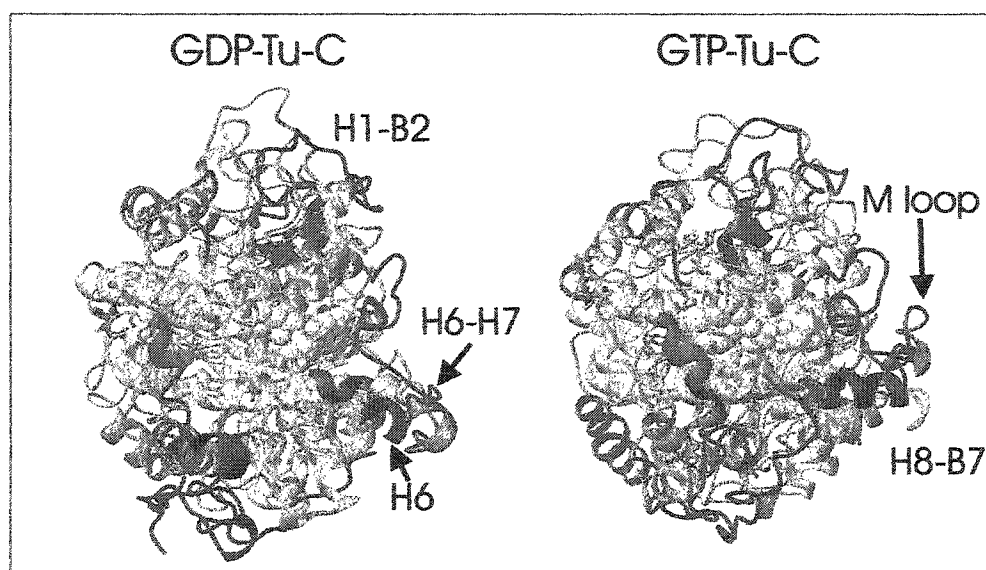
163 in αH4-B5 is involved in lateral contacts and is shown in ball and stick configuration in Figure 4.4. Its orientation with respect to the loop is variable. In GDP·Tu·C, it is pointing towards the outside of the MT and in GTP·Tu·C, it is pointing towards the inside of the MT. Loop αH8-B7 is on the side of the dimer and is coloured green in Figure 4.4. In GDP·Tu·C, the beginning of the loop is characterized by a dip towards the outside of the MT. This dip is not apparent in GTP·Tu·C. Loop αH9-B8 is coloured green in Figure 4.3. More of it is closer to the outside of the MT in GDP·Tu·C. Helix αH10 is yellow in Figures 4.3 and 4.4. It is more vertical in GTP·Tu·C and at an angle in GDP·Tu·C. This angle may account for the observed bending of GDP·Tu in disassembling MTs because H10 is involved in longitudinal contacts. This bending can put a strain on lateral contacts even though the residues directly involved in those have not shown significant movement in these simulations. Loop αH10-B9 is also yellow in Figures 4.3 and 4.4. It is further out than H10 in GTP·Tu·C but not in GDP·Tu·C. It should be noted that β tubulin has eight fewer residues than α-tubulin in the H10-B9 loop so the positions of the corresponding atoms is zero in the calculation for Figure 4.2.

There is a large amount of displacement between amino acids 300 and 350, the H9-B8 loop, B8, B8-H10 loop, H10, and the H10-B9 loop. When looking at the ribbon diagram of the final structure, one can see that the position of the C-terminus of α tubulin·C is vastly different with respect to this area. In GTP·Tu·C, the C-terminus has wrapped itself over the end of α tubulin·C coming into very close contact with these residues and in GDP·Tu·C, the C-terminus is folded in the opposite direction, towards β tubulin·C (see Figures 4.3 to 4.5). In β tubulin·C, this region is buried in the intradimer interface, explaining why the displacement is greater in α tubulin·C. The simulation results support the model in that the effect of hydrolysis on lateral contacts is mostly restricted to

β tubulin·C.

Loop βH3-B4, involved in intradimer contacts, is coloured blue in Figure 4.4. It appears to be more pinched in GDP·Tu·C. The end of βH6, βH6-H7 and the beginning of βH7 which are involved in lateral contacts are coloured blue in Figures 4.3 and 4.5. In Figure 4.3, βH6 is very disordered in GDP·Tu·C either influencing or influenced by the loop and βH7. In Figure 4.5, βH6 is very horizontal in GTP·Tu·C but is kinked downward in GDP·Tu·C. β tubulin's M loop is magenta in Figures 4.3 and 4.5. It is much closer to the outside of the MT in GDP·Tu·C. βB9-B10, on the inside of the MT and the taxotere binding region is coloured red in Figure 4.3 and seems to be slightly twisted in GTP·Tu·C. Loop βH11-H12, involved in longitudinal contacts, is blue in Figures 4.3 to 4.5. In Figure 4.5, it is at the front of the molecule and appears to go more to the left in GDP·Tu·C.

According to these results, the principles important for dynamic instability are at work here. In a B lattice described in Section 2.2.4, the lateral contacts between β tubulin·C seem to be strongly affected by the addition of the phosphate in the form of significant displacement of loop M. The lateral contacts between α monomers do not seem to be so obviously changed but the entire shape of the molecule is thinner laterally yet deeper from the inside to the outside of the MT (see Figure 4.5). This supports ideas that depolymerization of MTs stems from the weakening of lateral contacts and the release of the constrained GDP·Tu·C into its lower energy conformation. Lateral contacts may also be weakened by the change in angle of αH10. Since the carboxyl terminal regions seemed to greatly influence the structure of important binding regions of the dimer, the simulations were repeated for GTP·Tu·C and GDP·Tu·C without the C-terminal residues (Section 4.2) and a separate simulation was performed on the C-terminus alone when the dimer was in periodic boundary conditions to

imitate a MT lattice. (Section 4.3).

In Figure 4.5, GDP·Tu·C seems to be narrower laterally (in some areas) and thicker in the direction moving into or out of the center of a microtubule. The lateral dimension will be referred to as tubulin's width and the direction into or away from the center of the MT will be referred to as tubulin's depth for the course of this discussion. Assuming that hydrolysis of GTP when tubulin·C is within the MT lattice makes the configuration unstable, this instability may be partly due to a physical pulling of the GDP·Tu·C molecules against the lateral contacts in the lattice. Hydrolysis may even cause some lateral contacts to be broken.

Young's modulus for tubulin along the direction of a protofilament is known [22]. Using Hooke's law for solids, the energy due to stretching or compression of tubulin along its length, E, can be estimated using

$$E = \frac{Y}{2}\frac{\Delta l}{l_0}\Delta V = \frac{Y}{2}A\frac{(\Delta l)^2}{l_0} \tag{4.1}$$

if the dimer is approximated as a cylinder where Y is Young's modulus for tubulin, Δl is the difference in length between GTP and GDP tubulin·C, l_0 is the length of GTP·tubulin·C (i.e. before GTP hydrolysis) and A is the area of the end of the cylinder. In this case, the area is approximated by an ellipse whose principal axes are the depth and width of GTP·tubulin·C. The length, width and depth of tubulin were averaged over the molecule because the edges can be quite irregular. So, the length, width and depth of GTP·tubulin·C are 81.29Å, 39.92Å, and 45.66Å respectively. The corresponding dimensions for GDP·tubulin·C are 79.06Å, 41.02Å and 48.14Å respectively. Using these values, the energy involved in the compression after hydrolysis is 0.52eV, on the same order of magnitude as ATP hydrolysis energy. The change in length is also similar to what has been seen in experiment. Hyman *et al.* observed that the lattice spacing between
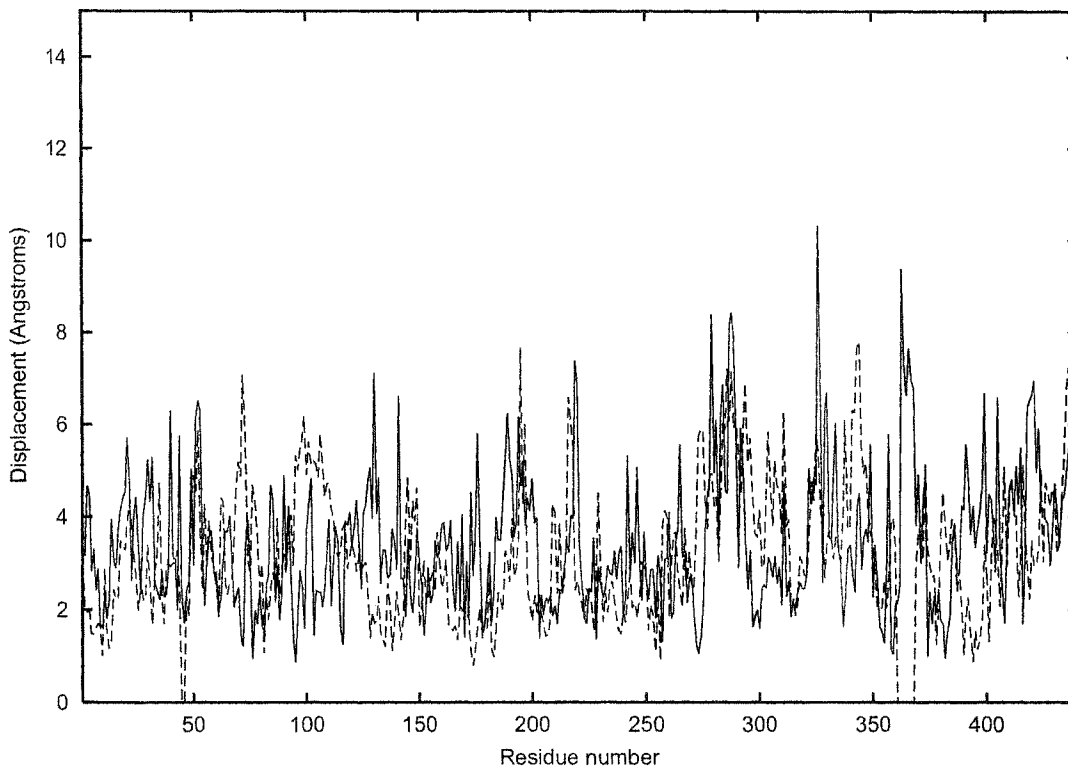
Figure 4.6: Displacement vs. residue number for GTP·Tu and GDP·Tu after simulated annealing. The solid line represents displacement for α tubulin·C and the dashed line is for β tubulin·C.

tubulin dimers with a nonhydrolyzable GTP analogue in a MT were longer in the x dimension by 1.5Å [23].

4.2 Simulations on Tubulin

As with tubulin·C, the stable regions of tubulin are generally the core β sheets of tubulin or loops and helices that are buried within the globular regions of the protein (see Table 4.4). In this case, stable is defined as having a displacement less than 3.4Å, the average displacement in Figure 4.6. Again. H1-B2 and H2-B3, were thus found to be stable. These two loops are in an area found by Nogales

Table 4.4: Stable regions in α and β tubulin, based on Figure 4.6. Regions in bold font are those that are not buried within the globular domain.

Residues	Structural Element(s)	Location
5-13	B1	β sheet 1
59-61	**end of H1-B2**	**inside of MT**
79-83	**beginning of H2-B3**	**inside of MT**
133-137	B4	β sheet 1
150-156	**H4**	**side of tubulin**
170-172	end of B5	β sheet 1
178-183	beginning of H5	buried, near nucleotide
203-208	end of B6, start of H6	buried
221-224	beginning of H7	buried
230-241	2nd half H7	buried
250-256	H8	buried
266-271	B7	β sheet 2
314-321	B8	β sheet 2
351-356	B9	β sheet 2
374-379	B10	β sheet 2
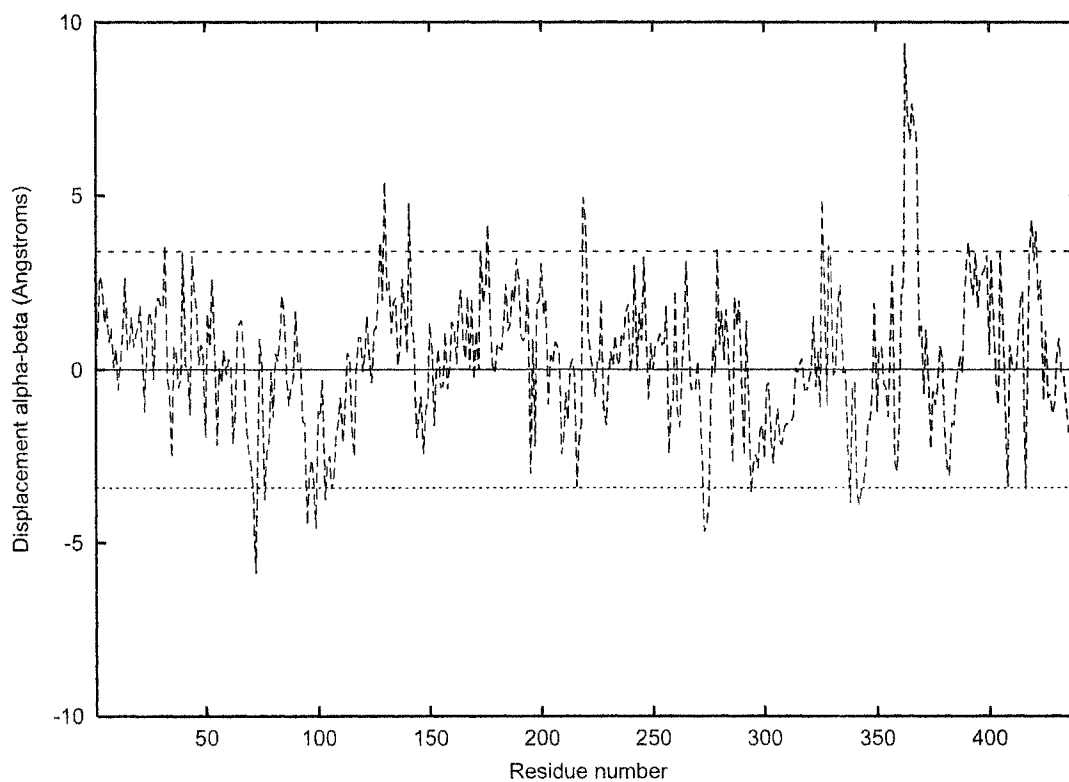
Figure 4.7: β-Tu displacement subtracted from α-Tu displacement of the data in Figure 4.6 so that negative values represent areas where β-Tu has moved more and positive values represent areas where α-Tu has moved more.

Table 4.5: Flexible regions in α tubulin only, based on peaks that are positive in Figure 4.7.

Residues	Structural Element(s)	Location
28-32	H1-B2	inside of MT
125-136	H3-B4	longitudinal contacts
137-143	B4-H4	buried, near GTP
173-177	B5-H5	buried, next to H11
219-222	H6-H7	lateral contacts
279	B7-H9 or M loop	lateral contacts
326-327,329-330	H10	lateral,longitudinal contacts
389-400	H11	outside of MT
418-423	end H11-H12	outside of MT

Table 4.6: Flexible regions in β tubulin only, based on peaks that are negative in Figure 4.7.

Residues	Structural Element(s)	Location
68-73	B2	buried
76-78	H2	inside of MT/end of molecule
93-102	B3-H3	longitudinal contacts
271-276	B7-H9 or M loop	lateral contacts
337-338,341-348	H10	lateral contacts
407-408, 416-417	H11-H12	longitudinal contacts

et al. to be quite flexible: the side facing the inside of the MT [35]. They must be kept stable by complicated interactions and need to be studied more closely in the presence of solvent.

Tables 4.5 and 4.6 show lists of peaks in Figure 4.7 where the difference between the displacements of α and β tubulin is greater than 3.4Å. Again, these tables show much more functional elements than Table 4.4 because the elements for the most part are on the outside faces of the molecule. H1-B2, B2, H2, B3-H3 and H3-B4 are all shared with tubulin·C. They are not necessarily flexible in the same monomer but this fact is a testament to the general flexibility of these elements.

From Tables 4.5 and 4.6, it is apparent that the differences between GTP·Tu and GDP·Tu are mainly in the most flexible regions of the protein: the loops on the outer surface of the molecule except for αB4-H4 and αB5-H5. Without the C-terminus α tubulin seems less stable. Figure 4.8 shows that the sheets are not as long or have broken up. Helices are kinked or partially unraveled. The differences between GTP·Tu and GDP·Tu after the simulation are due to partial denaturation causing irreversible disruption of structural elements, not conformational change. Conformational changes may also arise form many minute interactions transmitted from β-Tu to α-Tu. An exception in β-Tu is βB2. This area is coloured yellow in Figures 4.8 and 4.9. In both GDP·Tu and GTP·Tu, the β strand has become disordered enough not to be detected by MOLMOL's ribbon diagram program.

Regions labelled in Figures 4.8 to 4.11 are those that differ from the results obtained with tubulin·C. αH3-B4, involved in longitudinal contacts, is coloured orange in Figure 4.9. The part immediately after αH3 seems closer to the inside of the MT in GDP·Tu. αB4-H4 is coloured cyan in Figures 4.8, 4.9, and 4.11. In Figure 4.8 it is not visible in GTP·Tu because it is behind GTP (see Figure

4.9). In GTP·Tu (Figure 4.11), it is behind αH11, but in GDP·Tu is beside it. αB5-H5 is buried near αH11 and is pale green in Figures 4.8 and 4.11. In Figure 4.8, it reaches much more to the outside of the MT in GTP·Tu and in Figure 4.11, it is more to the side of the nucleotide in GDP·Tu than in GTP·Tu. Helix αH11 is coloured purple in Figures 4.8, 4.9, and 4.11. It appears to be generally disordered and unraveled in GDP·Tu.

Loop βB3-H3 is coloured red in Figure 4.10. It is involved in longitudinal contacts. In GTP·Tu, part of the loop goes in front of the phosphates but not so in GDP·Tu. Helix βH10 is pink in Figures 4.8, 4.10, and 4.11. This region is involved in lateral contacts and is kinked in GTP·Tu.

The M-loop is a prominent feature in both the α and β tubulin lines in Figure 4.6. The fact that this occurs for both monomers indicates that it is not a hydrolysis-induced change but rather brought about by the flexible nature of the loop, being quite long and on the outside of the molecule. H4 was also found to be stable in the previous simulation. The consistency of this element to be quite rigid implies some interaction with the stable part of the molecule keeping it in place. Even though it is on the surface of the dimer, it is backed by β sheet 1 and may interact with it. Other than a few exceptions, the stable regions of tubulin are as expected, the core of the globular domain while conformational changes are restricted to elements on the surface.

The subtle change in the local conditions caused by the absence of the C-terminii has held some elements more stable and allowed others to move more. In α tubulin, B4-H4, B5-H5, H11 and H12 all moved significantly even though they are not on the surface of the molecule. H11 is very close to H10 and B5-H5 so these regions may all affect one another. H12 moves when the C-terminii are not present so this outer region may act as a stabilizer for the outer helices.

Even in this simulation helix H3, which was proposed by Nogales to be a

Figure 4.8: GDP (top) and GTP (bottom) tubulin after simulated annealing. The side facing the inside of the MT is at the top. Regions of interest are coloured and labelled. Figure generated with MOLMOL [25].
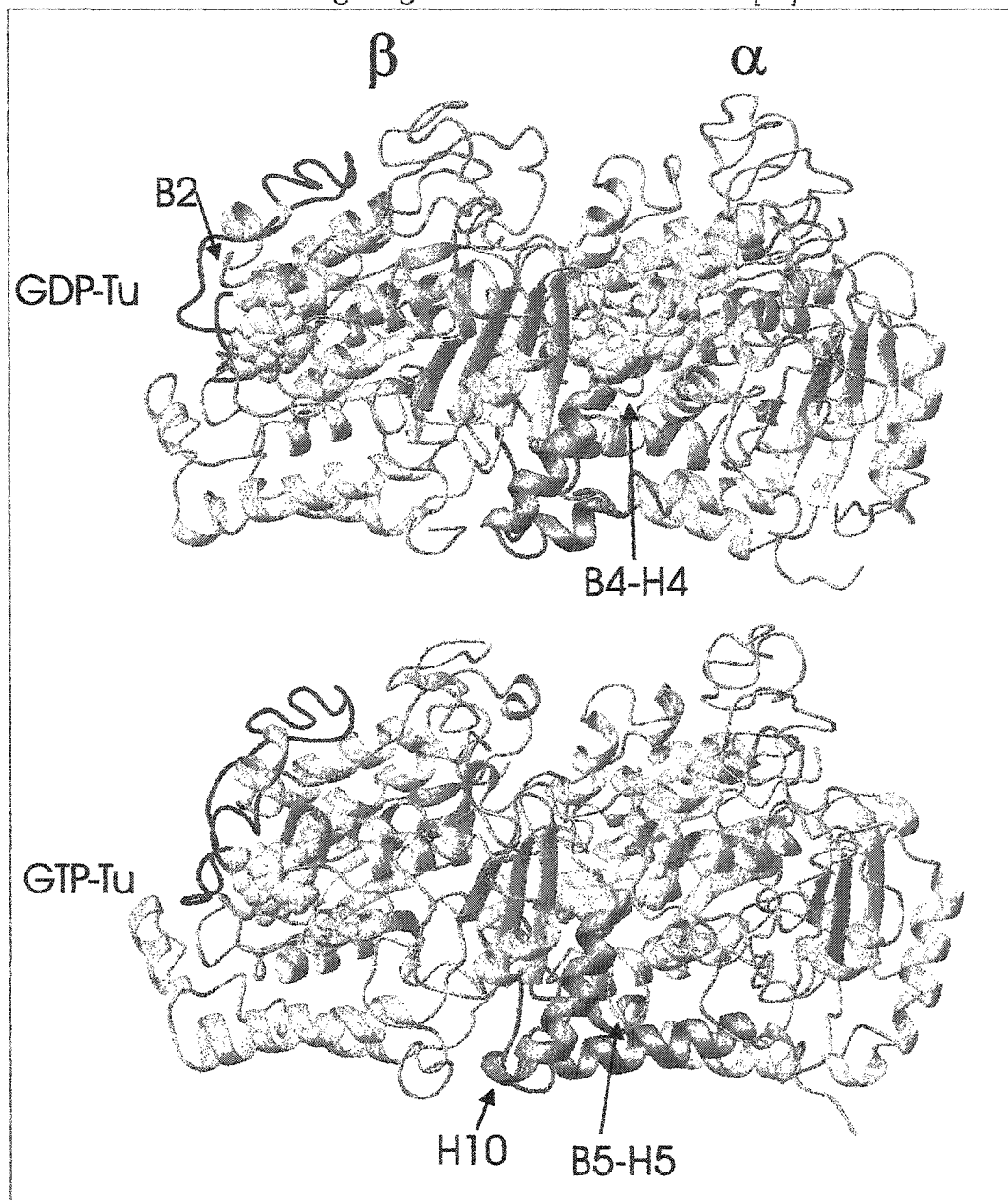
Figure 4.9: GDP (top) and GTP (bottom) tubulin from the opposite side after simulated annealing. The side facing the inside of the MT is at the top. Figure created using MOLMOL [25].
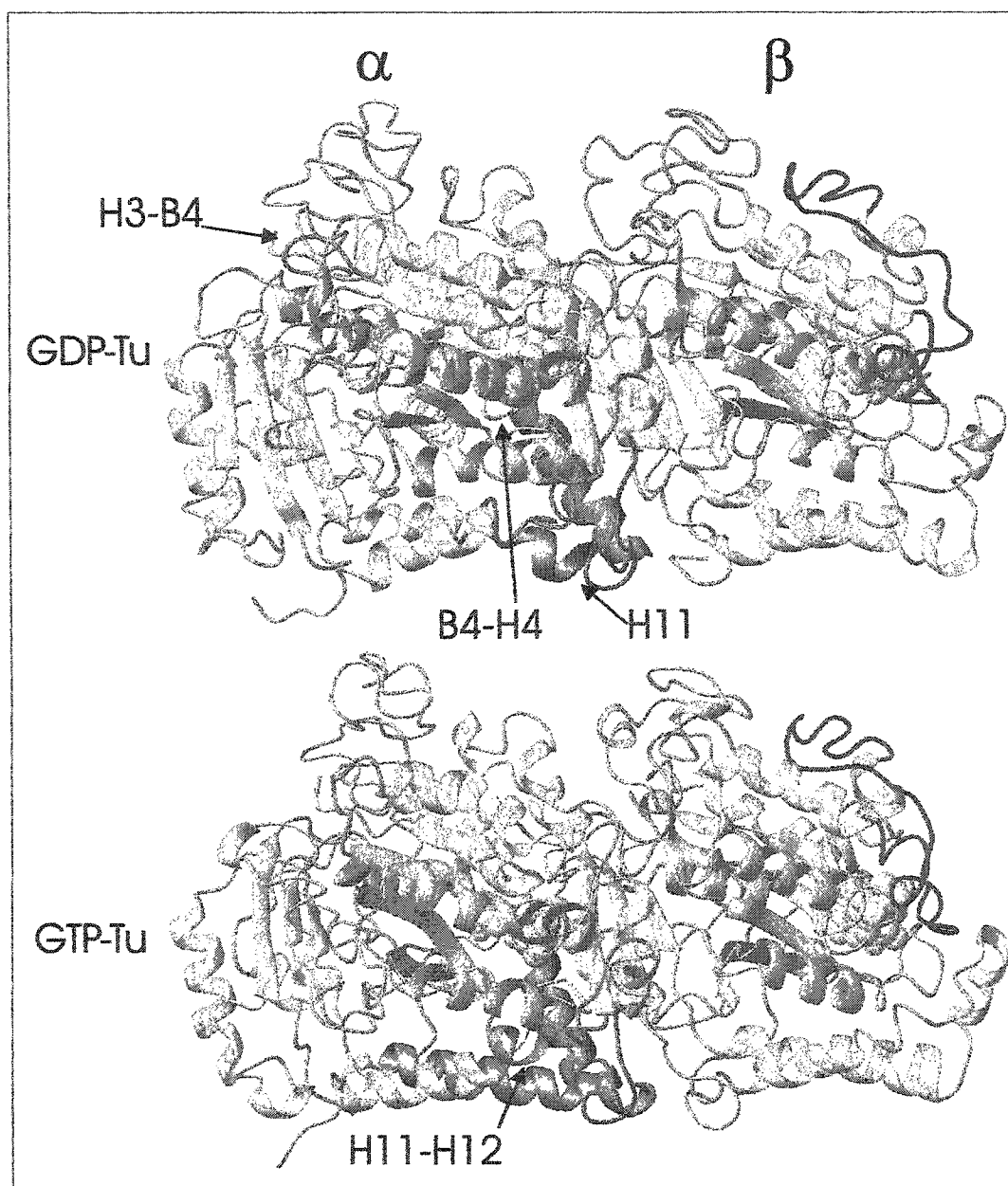
Figure 4.10: GDP (left) and GTP (right) tubulin looking at the β end of the molecule. The side facing the inside of the MT is at the top. Colouring is the same as in Figure 4.8 and this figure was again generated using MOLMOL [25].
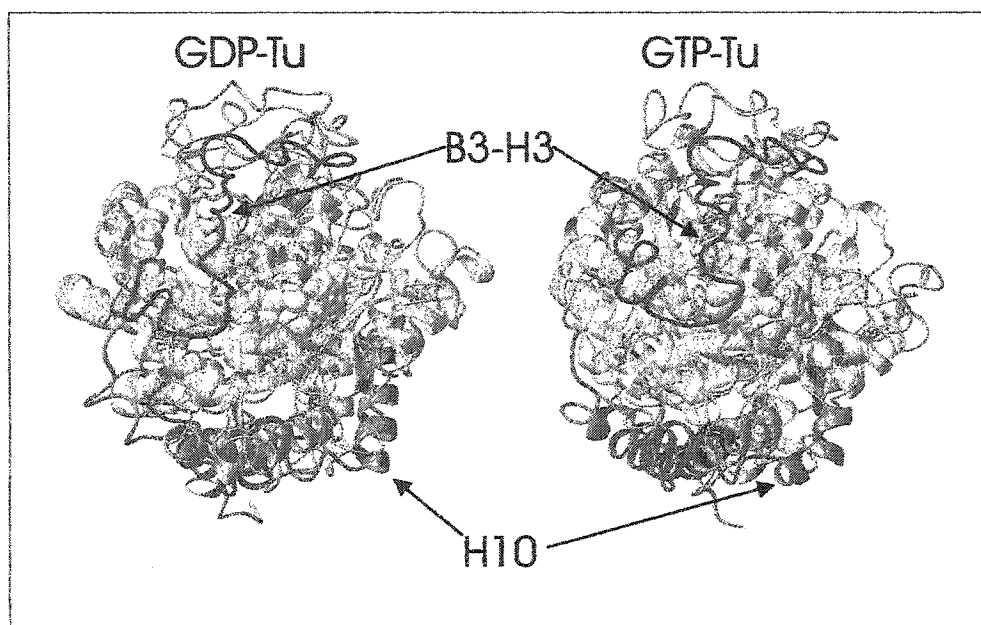
Figure 4.11: GDP (top) and GTP (bottom) tubulin from the outside of the MT after simulated annealing. This perspective looks at the side with the helices H11 and H12 and the C-terminus, had it been attached. Figure created using MOLMOL [25].
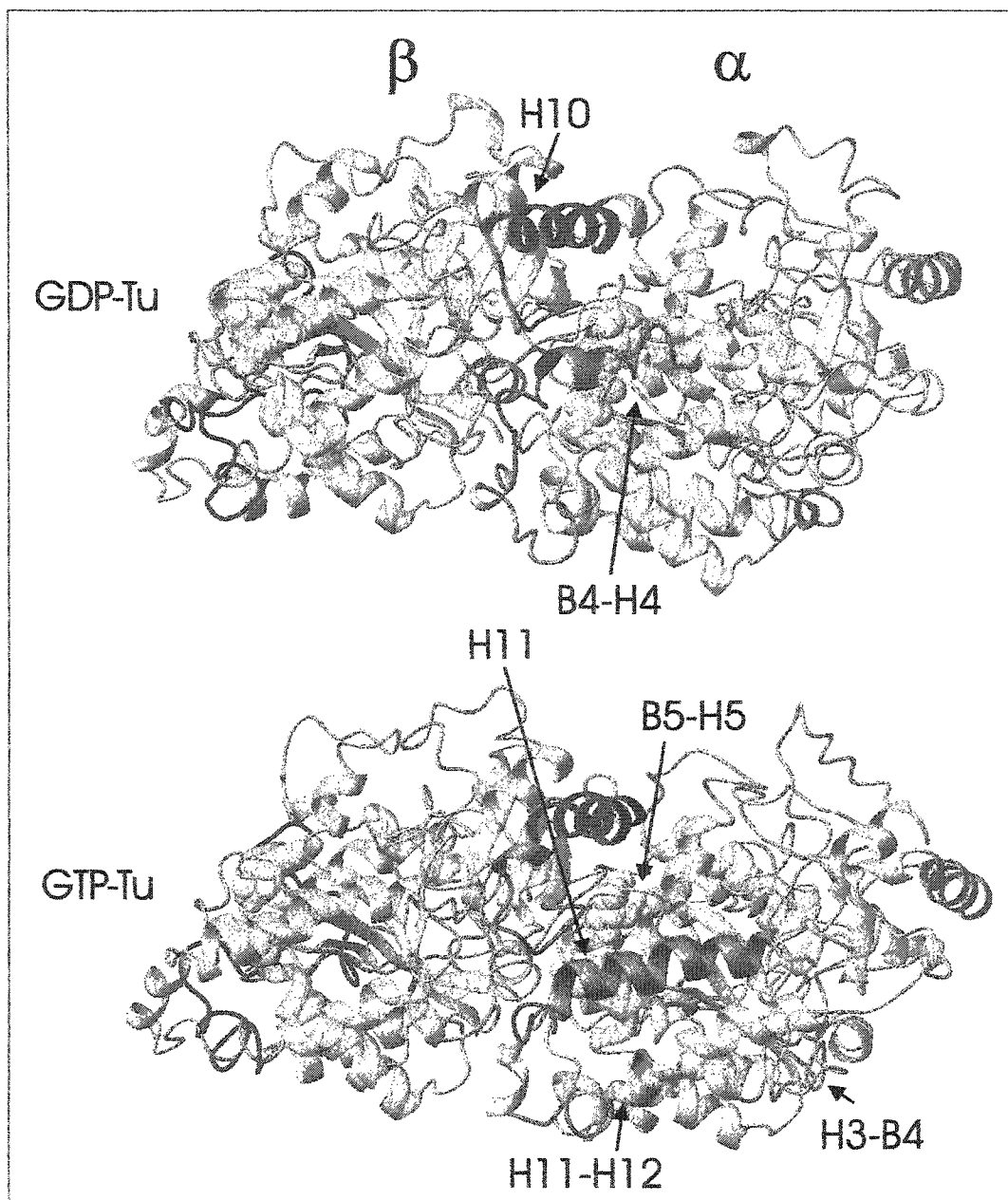
possible region for conformational change, was not observed to move much more than 3.4Å. The loop preceding this helix, B3-H3 has moved considerably in β tubulin. This loop has the potential to transmit a conformational change to H3 [34] but in Figure 4.8 this does not seem to have occurred. The same is true for helix H7 and loop H7-H8 [3,4].

The dimensions of GDP and GTP tubulin are 79.48 x 42.54 x 46.45 Å^3 and 78.2 x 39.71 x 45.04 Å^3, respectively. This time, the molecule is slightly longer when it contains GDP, not shorter. However, since this calculation was performed on free tubulin and the experiments in Hyman et al. [23] were done on tubulin in the MT lattice, certain differences in conformation are to be expected. Using equation (4.1), the energy of the elongation after hydrolysis is 0.17eV, also on the order of the energy of ATP hydrolysis.

4.3   Isolation of the Carboxyl Terminus

Anneal was run on GDP·Tu with only the carboxyl terminii (residues $\alpha436$-$\alpha451$ and $\beta427$-$\beta445$) allowed to move. Periodic boundary conditions were used so that the dimer was in a box 80Å by 46Å by 2000Å. An angle of 101.3099 degrees was imposed between the x and y axes of the periodic box to imitate the offset lattice configuration of a MT surface (Section 2.2.4).

When looking at Figure 4.12, there is a noticeable difference of position between the C-terminii from GDP and GTP tubulin. Since molecular dynamics simulations are deterministic, this effect comes solely from the presence or absence of the third phosphate in β tubulin. This effect is likely to be very small when the molecule is in solution. However, the configurations found here give three important pieces of information. First, that the negatively charged C-terminus is attracted to the body of the MT when no other more strongly positive molecules are present. Second, the different positions exemplify its flexibility

Figure 4.12: The C-terminii of GDP (green) and GTP (purple) tubulin after simulated annealing. In the top view the outside of the MT is at the top. The bottom view is from the outside of the MT. Figure created with MOLMOL [25].

and can be taken to be two possible configurations the C-terminii might adopt in vivo. In real systems, the influence of the single phosphate is likely to be small because of solvent effects and interaction of the C-terminus with motor proteins and other MT associated proteins. And third, Figure 4.12 shows the C-terminii from both α and β tubulin residing over the β monomer while the surface of the α monomer is exposed to the external environment. This is likely to have very important implications for proteins that bind to the surface of MTs.

4.3.1 Electrostatic Potential Between Tubulin and Kinesin

Conventional kinesin moves in only one direction along the MT: toward the plus end or away from the centrosome. In vivo, kinesin speeds range from 18nm/s (during mitosis and meiosis) to 2000nm/s in transport by flagella, along axons or in melanocytes. Conventional kinesin moves at approximately 1800nm/s. It is processive and can move along a MT surface for up to several microns, which equates to hundreds of steps. When kinesin tail regions are attached to a slide, the motor domains can move MTs as they hydrolyze ATP. Experiments have shown that increasing the number of kinesins linearly increases the rate of binding of MTs but does not affect the velocity of movement. Thus, kinesin's speed is independent of density and filament length. It takes exactly one step for each ATP hydrolyzed (at low loads) [27].

Motors bind in a specific orientation to filaments, and at a unique location. In the case of kinesin, neither of these has been unambiguously determined. The crystal structure of kinesin [26, 28] is of a form that is unbound to MTs and since kinesin's ATPase activity is MT-stimulated, kinesin likely changes conformation upon binding to the MT [22] Two examples can be found in Sosa *et al.* [38] and Hirose *et al.* [20, 21].

The results from the anneal simulations on the carboxyl terminii of GTP·Tu and GDP·Tu in Section 4.3 were used to calculate the electrostatic interaction potential between tubulin and kinesin. The potential was calculated as a function of x and y where x is the dimension running along the length of the MT towards the - end (i.e. from β to α along a tubulin dimer) and y runs along the width of the tubulin dimer. The orientation used is with the z axis running from the outside to the inside of the MT. ATP and ADP kinesin were used, in the conformations obtained after simulated annealing (Section 3.3). Figure 4.13 shows how kinesin was placed in the same orientation as in Sosa et $al.$ [38] -2Å from the outermost point of tubulin, on the side facing the outside of the MT. It was moved in x and y with 1Å resolution (see Figure 4.14). Since AMBER charge parameters were used, the potential was calculated with the electrostatic term from equation (3.4). A dielectric constant of 80.0 was used to provide appropriate damping of the electrostatic interactions due to water.

The results of these calculations are shown in Figures 4.15 to 4.18 and show that ADP kinesin has the greater affinity for tubulin. Whether tubulin had GTP or GDP in its E site, ADP kinesin was much more attracted to the MT surface than ATP kinesin. The minima of the graphs in Figures 4.15 to 4.18 are: -1.39eV for GDP·Tu and ADP·Kin; -0.47eV for GDP·Tu and ATP·Kin; -1.36eV for GTP·Tu and ADP·Kin and -0.46eV for GTP·Tu and ATP·Kin. The location of the minimum in Figures 4.15 and 4.17 are in roughly the same position as the location of the binding site found by docking calculations [3, 4]. This area also seems to be where the C-terminii have congregated, as seen in the bottom of Figure 4.12.

The difference in energies of the minima of ADP kinesin and ATP kinesin is -0.92eV (in the case of GDP·Tu), 2.73 times the energy released by ATP hydrolysis. This seems to come about because L11 of ATP·kinesin protrudes

Figure 4.13: Tubulin and kinesin with kinesin aligned as in Sosa *et al.* [38]. Kinesin, in blue, is at the top of the figure, on the outside of the MT. Tubulin is coloured grey with green C-terminii as in Figure 4.12. The MT plus end is at the left and the minus end is at the right. Figure generated with MOLMOL [25].
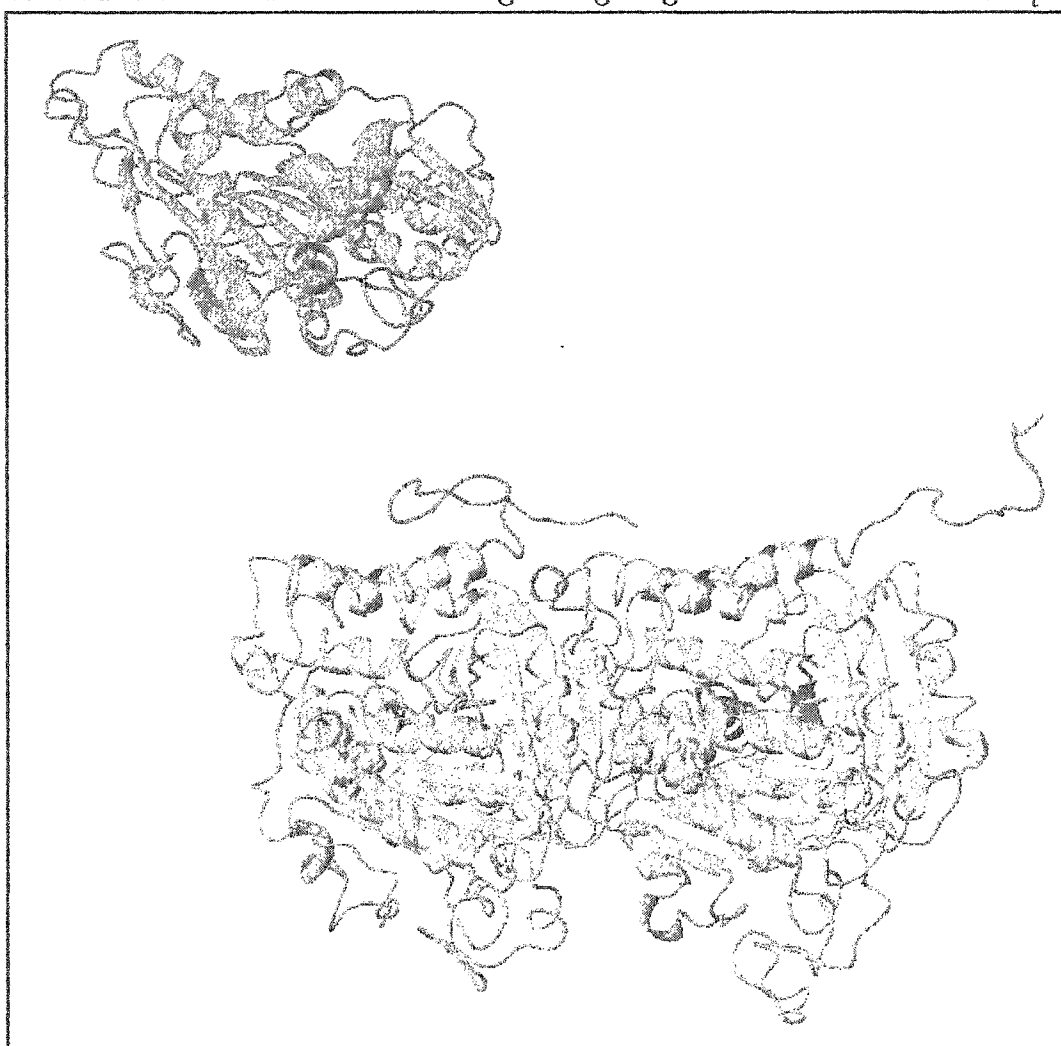
Figure 4.14: Map of kinesin movement over tubulin for the electrostatic potential calculation.
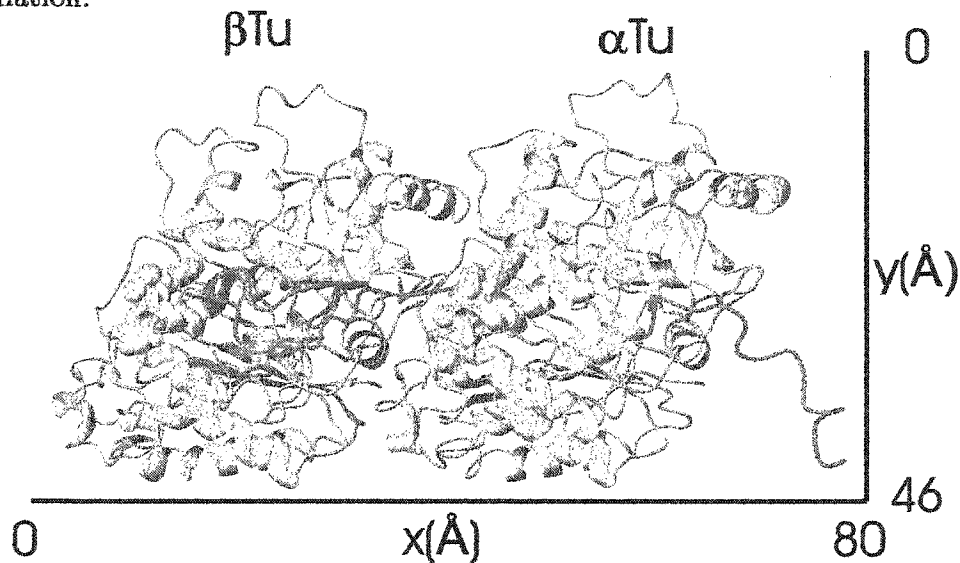
from the molecule towards tubulin. In order to get a 2Å separation between the two molecules, many of the positively charged lysine and arginine residues on kinesin's surface were further away from tubulin's negatively charged C-terminii than they were for ADP·Kin. While ATP·Kin may bind more strongly to MTs [44], ADP·Kin appears more likely to bind initially to the MT surface.

Figure 4.15: Electrostatic potential between GDP tubulin and ADP kinesin with respect to kinesin's position next to the tubulin dimer.
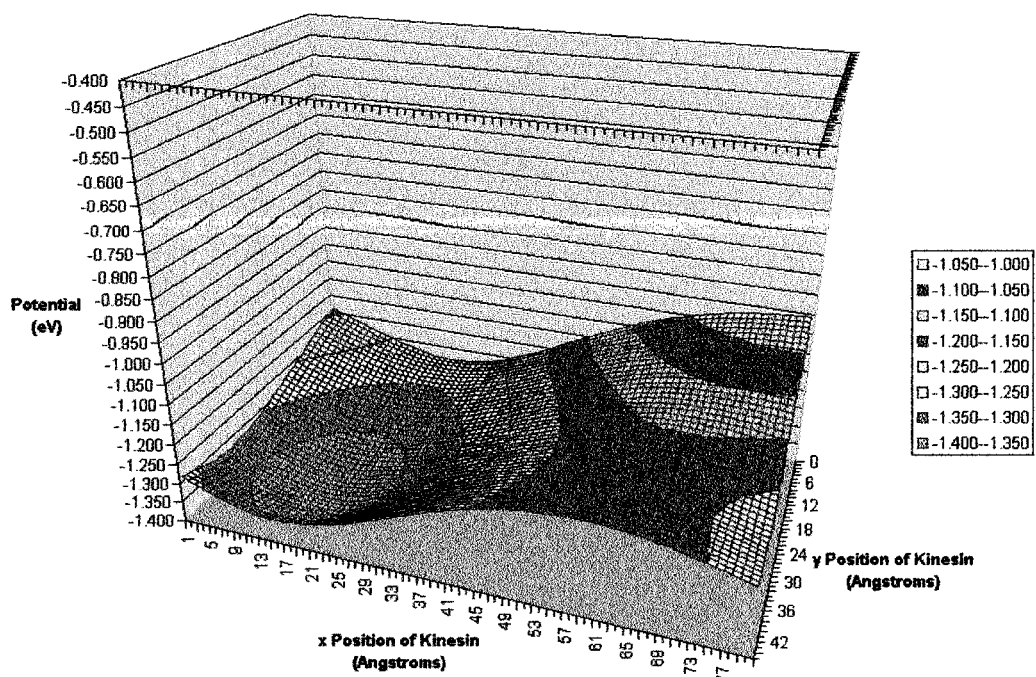
Figure 4.16: Electrostatic potential between GDP tubulin and ATP kinesin with respect to kinesin's position next to the tubulin dimer.
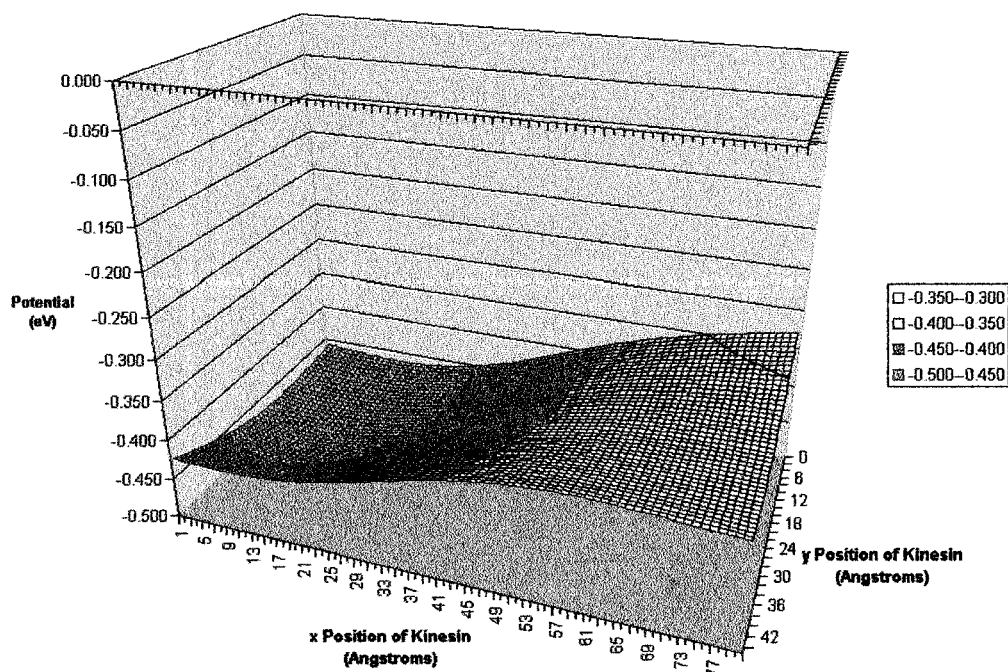
Figure 4.17: Electrostatic potential between GTP tubulin and ADP kinesin with respect to kinesin's position next to the tubulin dimer.
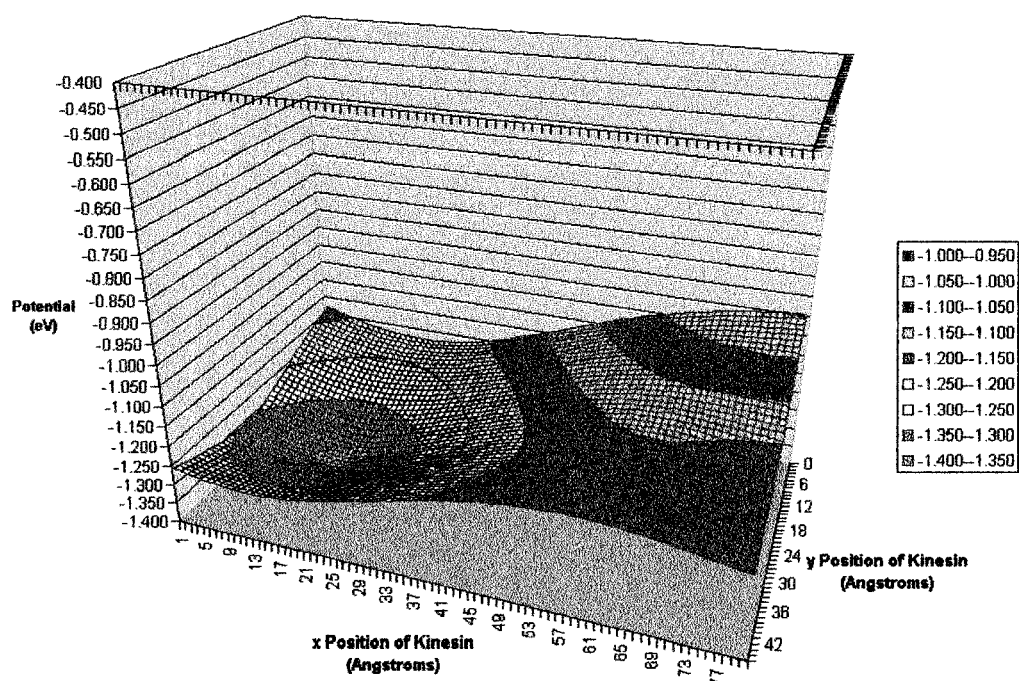
Figure 4.18: Electrostatic potential between GTP tubulin and ATP kinesin with respect to kinesin's position next to the tubulin dimer.
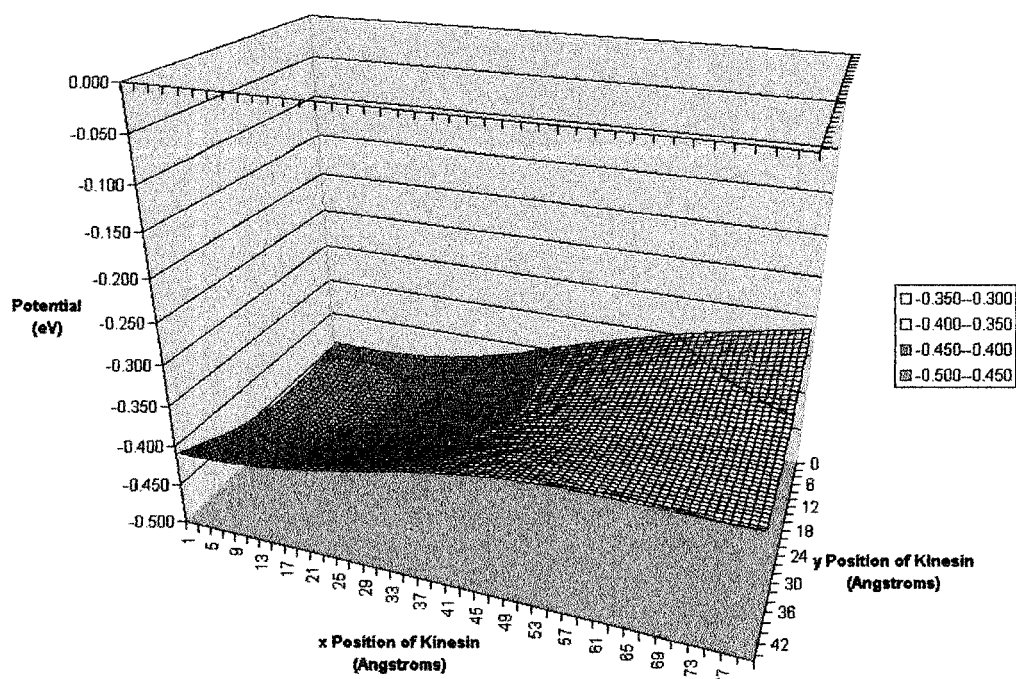
Chapter 5

Discussion and Conclusions

5.1   Simulated Annealing

The size of tubulin makes it difficult to study. In the simulations performed in the previous chapter, the number of elements that move is great and the nature of the movements is variable, be it a translation, a tilt, the development of a kink or any number of other movements. The interactions between various parts of the protein are also very complex and there is likely to be a multitude of them for any given helix, strand or loop. The observations already made are organized and studied in greater detail here.

5.1.1   Stable Elements in Both Tu and Tu·C

In general, tubulin·C and tubulin were both stable through the centers of the molecules, particularly the β sheets. None of the residues involved in longitudinal contacts were stable in both monomers which is not surprising since in the free tubulin dimer, these regions are in very different environments depending on which monomer they appertain to. Interestingly, tubulin·C had more stable regions that were on the outside of the globular domain than tubulin. Some

were involved in lateral contacts or on the side of the dimer such as H2-B3, B3-H3, H3, H4 and others were on the side facing the outside of the MT: H11 and H12. Only H2-B3 and H4 were also stable in tubulin without the C-terminii, a good indication that these structural elements are generally fixed in position. H4 and the stable lateral contacts H2-B3 and H3, are all on the same side of the dimer.

Helices H3 and H4 also contain numerous hydrophobic amino acids which may act as stabilizers. H3 has been named by Nogales *et al.* to be important in lateral contacts between tubulin·C dimers in the MT [34] and H4 is on the same side of the dimer but not explicitly involved in lateral contacts. However, since tubulin was in a vacuum for the simulation, these forces will have little effect. It is possible, however that the polar residues in these helices may be involved in electrostatic forces that keep them in place.

5.1.2 Flexible Elements in Both Tu and Tu·C

When comparing Tables 4.2 to 4.6, there is little consistency between the simulated annealing results on tubulin·C and tubulin. Only three structural elements move significantly in the same monomer in both simulations. B7-H9, or the M loop shows a lot of displacement in β tubulin both with and without the presence of the C-terminus. However, in the simulation without the C-terminii, this loop is present in the tables for both α and β tubulin. Different residues of the loop have moved in each monomer. This variation may be due to the flexibility of the M loop. In GTP·Tu (Figures 4.8 and 4.10) and GTP·Tu·C (Figures 4.3 and 4.5), this loop is in a very similar position. In GDP·Tu·C, the loop is much closer to the outside of the MT whereas in GDP·Tu, it seems to be drawing the loop closer to the body of the dimer. Perhaps for MT polymerization, the loop needs to be protruding from the outside of the dimer roughly halfway between the outside

and the inside of the MT as in Figure 4.5.

In tubulin·C, H10 has moved significantly only in α but is has moved in both monomers of tubulin. In tubulin·C, the C-terminus is affecting this region a great deal (Figure 4.3), but its location on the end of the dimer probably makes it quite mobile in general. There is also a possible relationship between the tilting of H10 in GDP·Tu·C and the observed ram's horn formation of protofilaments of disassembling MTs. H11-H12 underwent considerable movement in β tubulin in both simulations (Tables 4.3 and 4.6). In Figure 4.8 this region seems more disordered in GDP·Tu which may be less favourable for polymerization.

5.1.3   Discrepancies Between Tu and Tu·C

The regions that have moved only in the simulation without the C-terminii are all buried within the protein except for H12. This is consistent with the difficulties in starting this simulation because of certain regions becoming very disordered. Two atoms were held fixed during the simulation due to their tendency to cause disorder in the protein, even after the first minimization. The fact that H12 is in general less stable in tubulin than it is in tubulin·C suggests that the C-terminii have some kind of stabilizing influence on the surface of the dimer. Tubulin·C does have more stable regions that are on the outside of the molecule. H11 and H12 form the outer surface of the MT and their stability is likely to be important in MAP binding. Both these helices have at least one hydrophobic amino acid every third or fourth residue [35]. Since every turn of the α helix contains 3.6 amino acid residues [39], H11 and H12 have a hydrophobic interaction with the globular domain of the protein.

The remaining structural elements are those that were flexible in opposite monomers in tubulin and tubulin·C. H1-B2 is flexible in β tubulin·C and α tubulin. Since this region is such a long loop and has been observed to be

flexible before [35], this observation is likely simply due to the inherent flexibility of the element. The same can be said for H2, which is flexible in α tubulin·C and β tubulin. H3-B4, on the other hand is involved in longitudinal contacts. On β tubulin, it is in the intradimer interface and on α it is between dimers and possibly involved in the formation of MT protofilaments. In tubulin·C, this region was found to be flexible only in the β monomer and, in tubulin, it was found to be flexible only in α tubulin. It is also exposed to the inside of the MT and may be generally flexible and possibly influenced by H1-B2 which is also flexible in the corresponding monomers of tubulin·C and tubulin.

H6-H7 is flexible in β tubulin·C and α tubulin but is involved in lateral contacts. The regions should be in similar environments in both α and β tubulin and tubulin·C. However, this region is close to the α M loop and helix βH10, which are both flexible in tubulin. The loops probably all influence each other. This interaction would have been lessened had a solvent been included in the system.

H10-B9 is flexible in α tubulin·C and β tubulin. In tubulin·C, the α C-terminus is clearly interfering with this element (Figure 4.3). The same area in Figures 4.10 and 4.11, shows H10-B9 in β GTP·Tubulin being bent. It may be attracted to the disordered H11. Perhaps the C-terminus is required for the stability of these outer regions but if it moves a great deal, it can create more disorder.

5.1.4 Summary

The regions that H2-B3 and H3 bind to on the other side of the dimer, the M loop, H9-B8, H10, H6 and H6-H7, tend to be quite mobile. The flexibility of elements involved in contacts in MTs can explain how MTs are capable of having different numbers of protofilaments. One side may be designed for flexibility and the other

for stability because they are dominated by loops and helices, respectively (see Figure 2.6).

If the regions most likely to be definite conformational changes are those which were consistently flexible in the same monomers between tubulin and tubulin·C, the M loop, H10 and H11-H12 may have an influence on polymerization of tubulin dimers into MTs. Some theories of MT dynamics focus on lateral contacts [34], and others on longitudinal contacts [3]. From these findings it seems possible that both can be involved.

Any of the other observed flexibilities may be important but more tests need to be done to confirm results. One major improvement that can be made on the simulations would be to add solvent. In fact, the parameters in the AMBER force field were derived considering the use of an explicit solvent in simulations [9]. Wriggers and Schulten [44] added a coat of water molecules around the kinesin motor domain to achieve the effect of a solvent. Proteins do not function outside living systems where they are constantly in solution so to model them in vacuum is not realistic. However, given that the number of atoms in the tubulin system was at least 13852 and the anneal program required over 530 hours of computation time, performing anneal in vacuum was a necessary first step. A sheath of water molecules around tubulin would have dampened the attraction between the C-terminus and the globular region of the dimer in the first simulation. The final positions of many of the regions studied might have been very different if periodic boundary conditions had been added or if other dimers had been added to the system. In a MT lattice the C-terminus could not have embedded itself onto the side of tubulin·C. However, without the extra tubulin molecules, insight is gained into the conformation of free tubulin.

5.2 Tubulin-Kinesin Interaction

The exact mechanism of the processive motion of conventional kinesin is not yet fully understood, nor is the full interaction between kinesin and MTs known. As more data is collected including observations about the ATP hydrolysis cycle of kinesin, force and velocity measurements and crystallographic images of MTs decorated with kinesin, models come closer to completely describing the interaction. It is normal to refer to conventional kinesin simply as kinesin so for most of this section, the two terms will be interchangeable unless indicated otherwise.

5.2.1 Kinesin's ATP-hydrolysis cycle

In motor proteins the globular heads that interact with the filaments are where the hydrolysis cycle takes place so that it directly influences binding and unbinding from filaments. Conformational changes are projected further to create movement as well as binding/unbinding so that the protein may be displaced along the filament.

Hancock and Howard [18] found that the kinesin motor domain detached very slowly from MTs when it had ATP bound or when it contained no nucleotide. The ADP-bound and ADP·P-bound states detached much faster. Free kinesin (not associated with MTs) releases its phosphate very quickly as it has a high affinity for ADP [15]. The release of ADP is catalyzed by the binding of kinesin to the MT, it must lower the affinity kinesin has for ADP. Thus, the rate of ATP-hydrolysis is increased by 500 to $50s^{-1}$ in the presence of MTs (Hackney, 1995). There is also evidence that kinesin is folded over on itself when not bound to MTs, probably blocking the nucleotide binding domain [22]. This is further suggestion that the crystal structure of kinesin [26] could be very different from its MT-bound structure.

So, the hydrolysis cycle for one head is likely to be: (1) Kin·ADP binds to

the MT which causes the nucleotide to be released. (2) Due to increased affinity for ATP (by a factor of more than 10000) [22], kinesin binds ATP. (3) Hydrolysis occurs (this reaction is also accelerated by the MT) and then (4) Kin·ADP·P detaches from the MT. (5) Since free kinesin releases its phosphate quickly, the phosphate is released and (6) Kin·ADP binds to the MT. Step 6 is the same as step 1, completing the cycle. This is in accordance with the results obtained in the previous chapter showing that ADP·Kin was more attracted (by 2.73 times ATP hydrolysis energy) to tubulin than ATP·Kin. The protrusion of L11 in ATP·kinesin may allow it to bind more strongly to the MT than ADP·kinesin once the kinesin is already attached.

5.2.2   Kinesin's processivity

Conventional kinesin can travel for hundreds of steps before falling off the MT and to achieve this, it must be processive. The processivity is due to the fact that kinesin is attached to the MT during its rate-limiting steps: ADP release, ATP binding, hydrolysis but not phosphate release [22], which constitute a large portion of the time in one cycle bound to the MT. Experiments where a backwards force was applied to moving kinesin have shown that the motor protein spends no more than $1\mu s$ detached from the MT [30], which has led to the hand-over-hand mechanism where one head is always bound.

Evidence for processivity comes from motility assays and biochemical measurements. Motility assays have shown that kinesins can move MTs on slides even at very low kinesin concentrations over $1\mu m$ over 25s, which is roughly 125 molecules of ATP, given 1 molecule per 8nm step (Howard et al. 1989, Block et al. 1989, Coy et al. 1999). Biochemical measurements of the ATPase rate at low concentrations of tubulin being $5s^{-1}$ [16] back up this measurement. A large conformational change in kinesin is probably due to ATP binding in the

attached head [21]. Binding of ATP also accelerates binding of the free head to the MT, coupled to ADP release in that head. By this means, the hydrolysis cycles of the two heads can be coordinated.

When all this information is compiled, the cycle for two-headed processive kinesin is likely to be: (1) Kinesin with two ADP-bound heads is in the cytoplasm. (2) One head binds to the MT and subsequently loses its ADP. (3) The bound head gains an ATP and (4) hydrolysis of this ATP occurs causing the load and/or the unbound head to be moved towards the + end of the MT. (5) The free head's binding the MT is accelerated by this change and it binds to the next β-tubulin and in turn loses its ADP. (6) The first, now trailing, head has ADP·P bound and detaches from the MT and (7) releases its phosphate. At this point, the molecule has moved forward 8nm and the cycle can be repeated with the roles of the two heads reversed.

Models that accurately describe the motion of conventional kinesin must incorporate the coordination of the two heads, like Schief and Howard's hand-over-hand model [37]. According to this model, the release of the trailing head is contingent on the binding of the leading head [37]. The binding of the second head accelerates the normally slow detachment of the first head from the microtubule thus incorporating coordination between heads. The model predicts force velocity curves and step size as well as behaviour at very high load and low concentration of ATP that has not yet been experimentally verified [22].

5.3 Conclusions

There is still much more that can be done in terms of simulations on tubulin and kinesin. It would be interesting to perform the simulations on kinesin including at least part of the necklinker region to obtain insight into conversion of the conformational change to the location of the unbound head. Again, solvent

should be included at least around the C-terminii of tubulin and possibly around kinesin or filling the entire system. This will encourage appropriate hydrophilic and hydrophobic surface effects as well as appropriately damping the electrostatic potential between proteins and regions on the same protein. Periodic boundary conditions can be applied to tubulin while performing simulated annealing on the entire protein, not just the C-terminii. In addition, MD simulations on the C-terminii with kinesin or any other MAP in the vicinity may reveal more on that region's role in protein binding and its behaviour within the cell. Valuable insight has been gained here with respect to the flexibility of tubulin's M loop (especially when compared to the stability of H3) and its involvement in MT formation. Biochemical experiments that focus on this loop and other elements thought to be involved in interdimer contacts will provide an important verification of the predictions that modeling provides.

Bibliography

[1] B. Alberts, D. Bray, J. Lewis, M. Raff, K. Roberts, and J. D. Wilson. *Molecular Biology of the Cell*. Garland Publishing Inc., New York, third edition, 1994.

[2] R. A. Alberty and R. J. Silbey. *Physical Chemistry*. John Wiley & Sons, Inc., New York, first edition, 1992.

[3] L. A. Amos. Focusing-in on microtubules. *Curr. Opin. Struct. Biol.*, 10:236–241, 2000.

[4] L. A. Amos and J. Löwe. How does taxol stabilize microtubule structure? *Chemistry & Biology*, 6:R65–R69, 1999.

[5] D. Beeman. Some multistep methods for use in molecular dynamics calculations. *J. Comput. Phys.*, 20:130–139, 1976.

[6] P. R. Bergethon and E. R. Simons. *Biophysical Chemistry*. Springer-Verlag, New York, 1990.

[7] H. M. Berman, J. Westbrook, G. Gilliland Z. Feng, T. N. Bhat, H. Weissig, I. N. Shindyalov, and P. E. Bourne. The protein data bank. *Nucleic Acids Res.*, 28:235–242, 2000.

[8] S. M. Block. Leading the procession: New insights into kinesin motors. *J. Cell. Biol.*, 140(6):1281–1284, March 23 1998.

[9] J. F. Cannon. AMBER force-field parameters for guanosine triphosphate and its imido and methylene analogs. *J. Comp. Chem.*, 14:995–1005, 1993.

[10] R. B. Case, D. W. Pierce, N. Horn-Booher, C. L. Hart, and R. D. Vale. The directional preference of kinesin motors is specified by an element outside of the motor catalytic domain. *Cell*, 90:959–966, 1997.

[11] W. D. Cornell, P. Cieplak, C. I. Bayly, I. R. Gould, Jr. K. M. Merz, D. M. Ferguson, D. C. Spellmeyer, T. Fox, J. W. Caldwell, and P. A. Kollman. A second generation force field for the simulation of proteins, nucleic acids, and organic molecules. *J. Am. Chem. Soc.*, 117:5179–5197, 1995.

[12] A. Desai and T. J. Mitchison. Microtubule polymerization dynamics. *Annu. Rev. Cell Dev. Biol.*, 13:83–117, 1997.

[13] M. J. Dudek and J. W. Ponder. Accurate modeling of the intramolecular electrostatic energy of proteins. *J. Comput. Chem*, 16:791–816, 1995.

[14] D. K. Fygenson, E. Braun, and A. Libchaber. Phase diagram of microtubules. *Phys. Rev. E.*, 50:1579–1588, 1994.

[15] D. D. Hackney. Kinesin ATPase: Rate-limiting ADP release. *Proc. Natl. Acad. Sci. USA*, 85:6314–6318, 1988.

[16] D. D. Hackney. The rate-limiting step in microtubule-stimulated ATP hydrolysis by dimeric kinesin head domains occurs while bound to the microtubule. *J. Biol. Chem.*, 269:16508–16511, 1994.

[17] F. R. Hallett, R. H. Stinson, W. G. Graham, and P. A. Speight. *Physics for the Biological Sciences: A Topical Approach to Biophysical Concepts.* Concept Press, Toronto, second edition, 1992.

[18] W. O. Hancock and J. Howard. Kinesin's processivity results from mechanical and chemical coordination between the ATP hydrolysis cycles of the two motor domains. *P. Natl. Acad. Sci. USA*, 96(23):13147–13152, November 9 1999.

[19] U. Henningsen and M. Schliwa. Reversal in the direction of movement of a molecular motor. *Nature*, 389:93–95, 1997.

[20] K. Hirose, W. B. Amos, A. Lockhart, R. A. Cross, and L. A. Amos. Three-dimensional cryoelectron microscopy of the 16-protofilament microtubules: structure, polarity, and interaction with motor proteins. *J. Struct. Biol.*, 118:140–148, 1997.

[21] K. Hirose, J. Löwe, M. Alonso, R. A. Cross, and L. A. Amos. 3D electron microscopy of the interaction of kinesin with tubulin. *Cell Struct. Funct.*, 24:277–284, 1999.

[22] Jonathon Howard. *Mechanics of Motor Proteins and the Cytoskeleton.* Sinauer Associates, Inc., Sunderland, Massachusetts, February 2001.

[23] A. A. Hyman, D. Chrétien, I. Arnal, and R. H. Wade. Structural changes accompanying gtp hydrolysis in microtubules: Information from a slowly hydrolyzable analogue guanylyl-(α,β)-methylene-diphosphonate. *J. Cell Biol.*, 128(1-2):117–125, 1995.

[24] K. Kawaguchi and S. Ishiwata. Nucleotide-dependent single- to double-headed binding of kinesin. *Science*, 291:667–669, January 26 2001.

[25] R. Koradi, M. Billeter, and K. Wüthrich. MOLMOL: a program for display and analysis of macromolecular structures. *J. Mol. Graphics*, 14:51–55, 1996.

[26] F. Kozielski, S. Sack, A. Marx, M. Thormählen, E. Schönbrunn, V. Biou, A. Thompson, E.-M. Mandelkow, and E. Mandelkow. The crystal structure of dimeric kinesin and implications for microtubule-dependent motility. *Cell*, 91:985–994, December 26 1997.

[27] T. Kreis and R. Vale, editors. *Guidebook to the Cytoskeletal and Motor Proteins*. Oxford University Press Inc., New York, second edition, 1999.

[28] F. J. Kull, E. P. Sablin, R. Lau, R. J. Fletterick, and R. D. Vale. Crystal structure of the kinesin motor domain reveals a similarity to myosin. *Nature*, 380:550–555, April 11 1996.

[29] I. N. Levine. *Physical Chemistry*. McGraw-Hill Book Company, New York, third edition, 1988.

[30] Meyhöfer and J. Howard. The force generated by a single kinesin molecule against an elastic load. *Proc. Natl. Acad. Sci. USA*, 92:574 – 578, 1995.

[31] A. Mogilner, A. J. Fisher, and R. J. Baskin. Structural changes in the neck linker of kinesin explain the load dependence of the motor's mechanical cycle. *J. theor. biol.*, 211:134–157, 2001.

[32] E. Nogales. A structural view of microtubule dynamics. *Cell. Mol. Life Sci.*, 56:133–142, 1999.

[33] E. Nogales. Structural insights into microtubule function. *Annu. Rev. Biochem.*, 69:277–302, 2000.

[34] E. Nogales, M. Whittaker, R. A. Milligan, and K. H. Downing. High-resolution of the microtubule. *Cell*, 96:79–88, 1999.

[35] E. Nogales, S. G. Wolf, and K. H. Downing. Structure of the $\alpha\beta$ tubulin dimer by electron crystallography. *Nature*, 391:199–203. January 1998.

[36] D. L. Sackett. Structure and function in the tubulin dimer and the role of the acidic carboxyl terminus. *Subcellular Biochemistry – Proteins: Structure, Function and Engineering*, 24:255–302, 1995.

[37] Schief and J. Howard. Conformational changes during kinesin motility. *Curr. Opin. Cell. Biol.*, 13:19 – 28, 2001.

[38] H. Sosa, D. P. Dias, A. Hoenger, M. Whittaker, E. Wilson-Kubalek, E. Sablin, R. J. Fletterick, R. D. Vale, and R. A. Milligan. A model for the microtubules-ncd motor protein complex obtained by cryo-electron microscopy and image analysis. *Cell*, 90:217–224, 1997.

[39] L. Stryer. *Biochemistry*. W. H. Freeman and Company, fourth edition, 1995.

[40] K. Svoboda and S. M. Block. Force and velocity measured for single kinesin molecules. *Cell*, 77:773–784, June 3 1994.

[41] P. T. Tran, P. Joshi, and E. D. Salmon. How tubulin subunits are lost from the shortening ends of microtubules. *J. Struct. Biol.*, 118:107–118, 1997.

[42] P. T. Tran, R. A. Walker, and E. D. Salmon. A metastable intermediate state of microtubule dynamic instability that differs significantly between plus and minus ends. *J. Cell Biol.*, 138:105–117, 1997.

[43] W.F. van Gusteren and H. J. C. Berendsen. Computer simulation of molecular dynamics: Methodology, applications and perspectives in chemistry. *Angew. Chem. Int. Ed. Engl.*, 29:992–1023, 1990.

[44] W. Wriggers and K. Schulten. Nucleotide-dependent movements of the kinesin motor domain predicted by simulated annealing. *Biophys. J.*, 75:646–661, August 1998.